

MetaCLBench: Meta Continual Learning Benchmark on Resource-Constrained Edge Devices

Sijia Li^{1*}, Young D. Kwon^{2,3*}, Lik-Hang Lee⁴ and Pan Hui¹

¹HKUST

²University of Cambridge

³Samsung AI Center, Cambridge

⁴The Hong Kong Polytechnic University

sli308@connect.hkust-gz.edu.cn, ydk21@cam.ac.uk,

Abstract

1 Meta-Continual Learning (Meta-CL) has emerged
2 as a promising approach to minimize manual labeling
3 efforts and system resource requirements by enabling
4 Continual Learning (CL) with limited labeled samples.
5 However, while existing methods have shown success in image-based tasks, their effectiveness
6 remains unexplored for sequential time-series data from sensor systems, particularly audio inputs.
7 To address this gap, we conduct a comprehensive
8 benchmark study evaluating six representative Meta-CL
9 approaches using three network architectures on five datasets from both image and audio modalities.
10 We develop *MetaCLBench*, an end-to-end Meta-CL
11 benchmark framework for edge devices to evaluate
12 system overheads and investigate trade-offs among
13 performance, computational costs, and memory re-
14 quirements across various Meta-CL methods. Our
15 results reveal that while many Meta-CL methods en-
16 able to learn new classes for both image and audio
17 modalities, they impose significant computational
18 and memory costs on edge devices. Also, we find
19 that pre-training and meta-training procedures based
20 on source data before deployment improve Meta-CL
21 performance. Finally, to facilitate further research,
22 we provide practical guidelines for researchers and
23 machine learning practitioners implementing Meta-CL
24 on resource-constrained environments and make our
25 benchmark framework and tools publicly available,
26 enabling fair evaluation across both accuracy
27 and system-level metrics.

1 Introduction

31 With the popularization of artificial intelligence, the demand
32 for smart home technologies and voiceprint recognition is
33 increasing. Consequently, vision and audio-based applica-
34 tions such as image classification [Mai *et al.*, 2022], keyword
35 spotting (KWS) [Michieli *et al.*, 2023], and environmental
36 sound classification (ESC) [Chen *et al.*, 2022] have garnered
37 significant attention. However, these applications face a crit-
38 ical challenge: deployed models must continually learn and

40 update to accommodate new data and vocabulary as users' lin-
41 guistic patterns evolve with their environments [Marco *et al.*,
42 2024]. On resource-constrained edge devices, this adaptation
43 process often leads to the Catastrophic Forgetting (CF) prob-
44 lem [McCloskey and Cohen, 1989], where learning new tasks
45 (*e.g.*, words) compromises the model's ability to recognize
46 previously learned data.

47 Many studies have proposed addressing CF through Con-
48 tinual Learning (CL) methods, which enables learning of new
49 tasks with less forgetting [Shin *et al.*, 2017; Chaudhry *et al.*,
50 2019]. A multitude of CL methods have been proposed to
51 mitigate CF, including rehearsals-based approaches [Chauhan
52 *et al.*, 2020; Pellegrini *et al.*, 2020; Rebuffi *et al.*, 2017],
53 regularization-based methods [Kirkpatrick *et al.*, 2017; Zenke
54 *et al.*, 2017], and parameter isolation-based methods [Hung
55 *et al.*, 2019; Rusu *et al.*, 2016; Yoon *et al.*, 2017]. While
56 rehearsal-based approaches have demonstrated superior ac-
57 curacy in preventing forgetting [Kwon *et al.*, 2021a], they
58 demand substantial labeled data [Parisi *et al.*, 2019] and pose
59 significant memory and computational overheads for resource-
60 constrained devices.

61 To address these limitations, Meta-Continual Learning
62 (Meta-CL) has been introduced. It integrates few-shot learn-
63 ing into CL [Javed and White, 2019; Jerfel *et al.*, 2019] to
64 minimize the burden of manual labeling of conventional CL
65 methods and optimizes resource utilization through algorithm-
66 system co-design [Kwon *et al.*, 2024a]. Despite the benefits
67 of Meta-CL, there are still notable limitations that warrant
68 further investigation. First, the effectiveness of the existing
69 methods, which are typically used for tasks involving images,
70 has not been investigated fully with sequential time series
71 data provided by auditory sensor systems where the modality
72 of the data is significantly different from images [Purwins
73 *et al.*, 2019]. Second, the datasets tested have been rela-
74 tively simple and limited in its variety, consisting of a few
75 image/audio or specially crafted datasets that lack generaliz-
76 ability. Third, many existing studies [Javed and White, 2019;
77 Beaulieu *et al.*, 2020; Lee *et al.*, 2021] primarily focus on accu-
78 racy, neglecting crucial system requirements for edge devices,
79 potentially limiting their practical applicability.

80 In this paper, we address these gaps through a comprehen-
81 sive benchmark study of six representative Meta-CL methods
82 across three network architectures and five diverse datasets
83 spanning image and audio modalities. The employed methods

*Co-first authors

84 include regularization-based approaches ((1) Online aware
85 Meta-Learning (OML) [Javed and White, 2019], (2) A Neuro-
86 modulated Meta-Learning Algorithm (ANML) [Beaulieu *et*
87 *al.*, 2020], (3) OML with Attentive Independent Mechanisms
88 (OML+AIM), and (4) ANML with AIM (ANML+AIM) [Lee
89 *et al.*, 2021]) and rehearsal-based approaches ((5) Latent OML
90 and (6) LifeLearner [Kwon *et al.*, 2024a]).

91 While these methods have been largely evaluated in com-
92 puter vision applications utilizing Convolutional Neural Net-
93 work (CNN) architectures, their efficacy in processing au-
94 dio data and other architectures remains under-explored.
95 Hence, we adopted diverse audio datasets such as Urban-
96 Sound8K [Salamon *et al.*, 2014] and ESC50 [Piczak, 2015]
97 datasets for Environmental Sound Classification and the
98 GSCv2 [Warden, 2018] dataset for keyword spotting (KWS).
99 Furthermore, we incorporated two commonly used image
100 datasets such as MiniImageNet [Vinyals *et al.*, 2016] and
101 CIFAR-100 [Krizhevsky *et al.*, 2009] to compare the effective-
102 ness of Meta-CL on image datasets versus audio datasets.

103 Previous studies [Beaulieu *et al.*, 2020; Lee *et al.*, 2021;
104 Kwon *et al.*, 2024a] have exclusively evaluated simple three-
105 layer CNN architectures for Meta-CL. To bridge this research
106 gap, we incorporated MobileNet-based architecture, YAM-
107 Net [Howard *et al.*, 2017], capable of recognizing audio
108 events. We also employed Vision Transformers (ViT) archi-
109 tecture [Dosovitskiy *et al.*, 2020] for images to conduct a
110 comparative study.

111 Overall, we make the following key contributions.

- **Comprehensive Evaluation Framework** (Section 3): We developed *MetaCLBench*, an end-to-end benchmark framework that incorporates diverse audio (GSCV2, UrbanSound8K, ESC50) and visual datasets (CIFAR100, MiniImageNet), enabling thorough evaluation across different data modalities. The framework assesses both accuracy and system-level metrics, including computational efficiency, memory and energy consumption. Also, our evaluation covers multiple architectures of varying complexity, offering a robust understanding of Meta-CL performance across different computational scenarios.
- **Empirical Insights** (Section 4): We present comprehensive findings demonstrating the effectiveness of Meta-CL methods across both image and audio domains. Our analysis quantifies the computational and memory demands on edge devices (Section 4.1), while revealing that pre-training and meta-training procedures significantly enhance Meta-CL performance during deployment (Section 4.2). Notably, we find that well-tuned basic 3-layer CNN architecture with proper pre-training can outperform more sophisticated models such as ViT and YAM-Net (Table 1) under difficult Meta-CL setups, challenging conventional assumptions about model complexity.
- **Open Resources and Practical Guidelines** (Section 5): By implementing *MetaCLBench* on edge devices, we provide realistic insights and practical guidelines specifically tailored for resource-constrained devices. Furthermore, we plan to release our benchmark framework and evalua-

tion tools¹ to enable fair and comprehensive assessment of both accuracy and system-level performance metrics. This will facilitate reproducible research and accelerate the development of practical Meta-CL solutions for real-world applications.

2 Related Work

Continual Learning: CL aims to assimilate new knowledge in dynamically evolving input domains through progressive acquisition [Mai *et al.*, 2022; Wang *et al.*, 2024]. When algorithms are trained sequentially, the new learning will interfere with previous established weights, leading to CF of the previous learning [McCloskey and Cohen, 1989]. Current CL approaches to the CF challenge can be divided into two categories based on task information management. The first approach incorporates regularization terms into the loss function to facilitate knowledge of old and new models, thereby preserving previously learned knowledge [Rannen *et al.*, 2017; Li and Hoiem, 2018; Rodríguez *et al.*, 2021; Ahn *et al.*, 2019]. The second approach involves either original or pseudo-samples from previous tasks during new task training [Shin *et al.*, 2017; Rolnick *et al.*, 2019; Chaudhry *et al.*, 2019].

Meta Continual Learning: Meta-CL updates the model in the outer loop using learned random samples and optimizes it in the inner loop with a few samples before passing it to the outer loop [Jerfel *et al.*, 2019]. Previous research on Meta-CL has primarily concentrated on image recognition applications. Online-aware Meta-Learning (OML) [Javed and White, 2019] and A Neuromodulated Meta-Learning (ANML) [Beaulieu *et al.*, 2020] both demonstrated high CL performance on the Omniglot dataset [Lake *et al.*, 2015]. Based on these approaches, state-of-the-art (SOTA) Meta-CL incorporated the Attentive Independent Mechanisms (AIM) module, which can independently acquire new knowledge to enhance model performance [Lee *et al.*, 2021]. However, due to its high processing cost, using Meta-CL is challenging on low-end edge devices [Kwon *et al.*, 2024a]. LifeLearner addresses these limitations by integrating meta-learning, rehearsal mechanisms, and resource-efficient compression, making it suitable for deploying Meta-CL applications on resource-constrained devices [Kwon *et al.*, 2024a].

Continual Learning for Image and Audio Applications: CL has remarkable capabilities in sensing applications, including action recognition, audio sensing, and speech recognition [Jha *et al.*, 2021; Kwon *et al.*, 2021a]. Its ability to update models based on continuous data streams makes it particularly valuable for mobile devices processing speech and image data. Researchers have successfully applied CL to speech and emotion recognition [Thuseethan *et al.*, 2021]. CL systems integrated into edge devices with audio and microphones continually learn from ambient human voices and environmental sounds to improve recognition accuracy [Kwon *et al.*, 2021b]. In image recognition, CL facilitates applications such as food recognition [He and Zhu, 2021], where systems must continuously learn from new instances to enhance recognition accuracy.

¹<https://github.com/theyoungkwon/MetaCLBench>

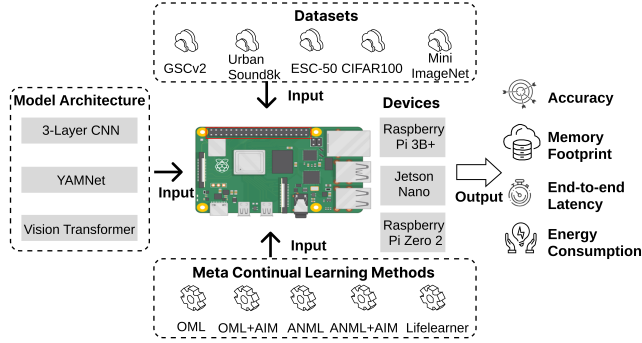


Figure 1: The framework overview. Testing trade-offs between performance and system resources across three devices with five datasets and six Meta-CL methods using three model architectures

In contrast to these real-world applications, our study explores CL’s capability to optimize the trade-off between performance and system resources on resource-constrained edge devices. We comprehensively evaluate five Meta-CL methods across image and audio domains using various architectures ranging from 3-layer CNN, YAMNet, to ViT, accounting for the unique characteristics of each modality and architecture.

3 Benchmark Framework

3.1 Continual Learning Task

Problem Formulation: CL addresses the challenge of learning new tasks without forgetting previously learned ones. Given a sequence of tasks S , the objective is to maintain robust performance across all tasks $S_{1,\dots,n}$. Our evaluation framework encompasses $(T(Task), S(Sequence), D(Datasets))$, where each task represents a distinct sound class. Each subsequent task S_n is derived from the historical training records of the most recent sets $S_{n-1}, S_{n-2} \dots S_{n-m}$ of the employed audio and image datasets.

Meta-Learning is conducted in both the inner and outer loops, enabling the training of each inner loop round through the outer loop. Each inner loop iteration is performing a complete learning process, evaluating both the acquisition of new tasks and the retention of previously learned ones. The meta-loss gradient (comprising newly learned errors and errors from random sampling of the dataset) propagates back to update the initial parameters. This process continues iteratively as new tasks are incorporated. By constraining each inner loop to a single new task while continuously undergoes meta-training, it mitigates CF and optimizing computational efficiency.

Our Framework Overview: Figure 1 shows our experimental framework, *MetaCLBench*, designed to evaluate the performance and resource trade-offs across multiple dimensions: three devices, five datasets, six Meta-CL methods, and three architectures. *MetaCLBench* extends Meta-CL by implementing a comprehensive evaluation system that spans multiple modalities and practical considerations. By combining both visual and audio datasets, we provide thorough insights into Meta-CL performance across diverse data types. We conduct a detailed system-level analysis of computational efficiency, memory usage, and energy consumption, partic-

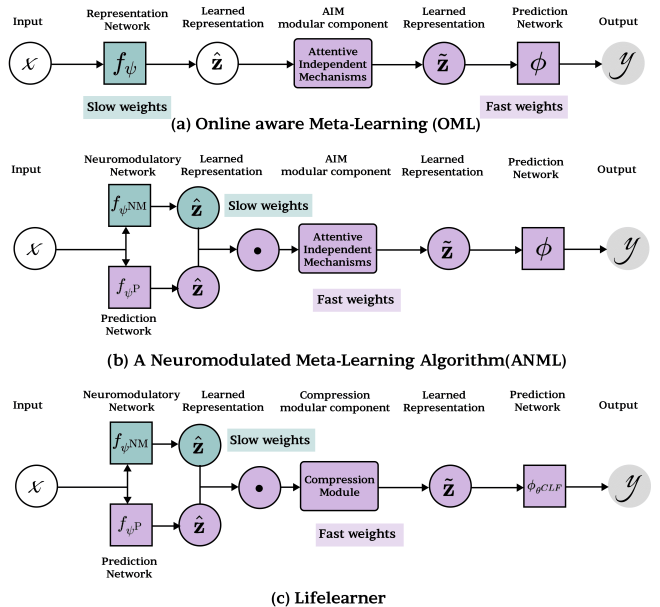


Figure 2: The illustration of the Meta-CL methods evaluated in our benchmark framework.

ularly on resource-constrained edge devices for real-world applications. Overall, our framework evaluates six established Meta-CL methods across three network architectures of varying complexity, creating a robust benchmark framework that assesses both theoretical capabilities and practical constraints. We now explain each of the components of our framework in the following subsections.

3.2 Meta-CL Methods

Figure 2 presents six distinct Meta-CL methods: Online aware Meta-Learning (OML), OML with Attentive Independent Mechanisms (OML+AIM), A Neuromodulated Meta-Learning Algorithm (ANML), ANML+AIM, and LifeLearner. The following sections detail each method.

OML [Javed and White, 2019]: This is an approach that continuously optimizes representations during online updates to quickly acquire predictions for new tasks, facilitating seamless and efficient CL. This approach uses CF as signals to justify the use of storage space for accommodating new tasks. The OML can accomplish CL in more than 200 consecutive classes. It is an online updating method that constantly learns representations and often outperforms rehearsal-based continual learning methods.

ANML [Beaulieu et al., 2020]: This is an approach inspired by the neuromodulation process in the brain. This method accomplishes selective activation (forward pass) and selective plasticity (backward pass) in DNNs by meta-learning through a CL process within the prediction network (f_ϕ). Optimizing activation timing by controlling the activation of a predictive model based on input conditions enhances continual learning. It is often reported to be superior to OML, as it can be optimized to reduce both forward and backward interference.

OML+AIM [Lee et al., 2021]: This is a Meta-CL approach that integrates Attentive Independent Mechanisms (AIM),

which is a modular component into OML framework. AIM increases the speed of learning a new task by selecting out the mechanism that best explains the representation of the inner loop to activate.

ANML+AIM [Lee et al., 2021]: This is a Meta-CL approach that incorporates AIM into ANML framework. The accuracy of SOTA Meta-CL continues to improve beyond the performance of the previous three approaches by integrating AIM into the existing CL framework.

LifeLearner [Kwon et al., 2024a]: This module is based on ANML and combines both lossy and lossless compression to achieve high compression rates and minimize footprint. The LifeLearner approach not only achieves optimal CL efficiency but also significantly reduces energy consumption and latency compared to the SOTA. And it achieves efficient learning even on resource-constrained edge devices.

Latent OML: This module is based on OML and incorporates the rehearsal strategy from LifeLearner to achieve high Meta-CL accuracy. It is used to evaluate advanced architectures (YAMNet and ViT).

3.3 Datasets

Google Speech Commands V2 (GSCV2) [Warden, 2018] is a massive database of one-second voice clips of 30 short words consisting of a solitary spoken English word or ambient noise divided into 35 classes with 105,829 clips. These clips are derived from a limited number of commands and are spoken by various speakers. Each class has 2,424 input data for training and 314 for testing, with 25 classes allocated for meta-training and the remaining 10 for meta-testing. Then, up to 30 samples are provided for each class during meta-testing.

Urbansound8k is a comprehensive collection for environment sound classification (ESC) applications comprising 8,732 labeled sounds that are no more than four seconds [Salamon et al., 2014]. This single-labeled dataset is categorized into ten classes from the taxonomy in real-world settings, including children playing sound, street music, gunshots, etc. Referring to previous studies [Su et al., 2019], indicate that four features in each audio clip were extracted and resampled to 22 kHz. Among the ten classes, half of them are allocated for meta-training, while the other half are specifically assigned for meta-testing. Up to 30 samples are given for each class during the meta-testing. Based on the first three seconds of each audio segment, the input to the audio is 128×85 (*number of frames*) \times 85 (*size of the set of four features*).

ESC50 is a smaller volume collection consisting of 2,000 environment sounds in 5-second segments [Piczak, 2015]. This single-labeled dataset is categorized into 50 classes and divided into five groups: animals, natural soundscapes, human sound without speech, domestic sounds and urban noises. Out of the 50 classes. 30 are designated for meta-training and the remaining 20 for meta-testing. Then, up to 30 samples are given for each class during meta-testing. As part of the preprocessing procedure, we resampled the ESC50 samples to 32kHz and generated an input with dimensions of 157×64 (*number of frames*) \times 64 (*features*) [Chen et al., 2022; Pons et al., 2019].

CIFAR-100 consists of 60,000 images distributed across 100 classes and is widely used for training and assessing var-

ious machine learning algorithms in tasks related to image classification [Krizhevsky et al., 2009]. Each class contains 500 photographs for training and 100 images for testing. Of the 100 classes, 70 are designated for meta-training and 30 for meta-testing. In both phases, 30 random training images per class are utilized. For the meta-testing phase, 900 samples are utilized during meta-testing to carry out CL.

MiniImageNet is excerpted from the Imagenet dataset and is utilized in few-shot learning research [Vinyals et al., 2016]. Based on the previous research, the MiniImageNet dataset is composed of 64 classes designated for meta-training and 20 for meta-testing. Each class offers 540 images for training and 60 for testing. Moreover, a total of 600 samples are available during the meta-testing phase.

3.4 Model Architecture

We augmented the 3-layer CNN architecture previously employed in CL studies by incorporating the YAMNet network architecture with pre-training. In addition to assessing YAMNet as a model for the speech domain with pre-training, we also evaluated the ViT, a transformer model that integrates a pre-trained model used for image classification by segmenting the image to a fixed size for input to the transformer encoder.

3-layer Architecture: The methods depicted in Fig. 2 consist of feature extractors and classifiers. The feature extractor transmits the learned features to the AIM and the compression modules, followed by classification. The $f_\varphi W$ added to the AIM module components can be used to minimize forgetting and learn new categories efficiently. In the 3-layer architecture, the feature extractor for OML and OML+AIM incorporates f_φ , which is a 6-layer CNN with 112 channels, and the classifier has two fully-connected layers. And the LifeLearner and ANML+AIM share the same natural structure. The feature extractor includes a neuromodulatory network ($f_{\varphi NM}$) and a prediction network ($f_{\varphi P}$), which is a 3-layer CNN with 112 channels. The classifier consists of a single fully-connected layer with 256 channels.

YAMNet [Howard et al., 2017] employs the MobileNetV1, which features a depthwise separable convolution architecture designed to decrease model size and latency and a full convolution on the first layer. The depthwise separable convolution comprises a deep convolution responsible for filtering and a pointwise convolution used 1×1 convolution responsible for combining features, effectively mixing information from all output channels in the deep convolution step. MobileNetV1 consists of 28 layers, with each layer being downsampled through strided convolution. Additionally, MobileNets introduces two hyperparameters, a width multiplier and a resolution multiplier, which facilitate the balance latency and accuracy.

ViT [Dosovitskiy et al., 2020] embodies a hybrid architecture. Since ViT only has a Multilayer Perceptron (MLP) layer with localization and translation equivalence, the image-specific generalization bias of ViT is much smaller than that of CNN. The same five methodologies deployed in the 3-layer architecture have been adapted for use with ViT. ViT begins by partitioning an image into patches; these patches, extracted from the CNN feature maps, serve as alternative input sequences for the model.

3.5 System Implementation

The implementation of our benchmark framework, *MetaCLBench*, consists of two stages. We developed the first stage, pre-training and meta-training, of Meta CL methods on a Linux server to initialize and optimize neural weights in order to enable fast adaptation during deployment scenarios with a few samples. After that, we implemented the second stage, meta-testing (i.e., actual deployment setup), on our target devices: (1) embedded and mobile systems such as Jetson Nano and Raspberry Pi 3B+ and (2) a severely resource-constrained IoT device like Raspberry Pi Zero 2. In addition, for methods that utilize hardware-friendly optimization (e.g., LifeLearner), we also adopt their optimization techniques in our framework. Specifically, *MetaCLBench* incorporates hardware-friendly 8-bit integer arithmetic [Jacob *et al.*, 2018] which reduces the precision of weights/activations of the model from 32-bit floats to 8-bit integers, increasing the computation throughput and minimizing latency and energy. *MetaCLBench* uses the scalar quantization scheme [Jacob *et al.*, 2018] to minimize the information loss in quantization. Also, the QNNPACK backend engine is used to execute the quantized model on the embedded devices.

Embedded Devices: *MetaCLBench* employs three diverse edge devices: (1) Jetson Nano, (2) Raspberry Pi 3B+, and (3) Raspberry Pi Zero 2 which are equipped with a quad-core ARM processor and 4 GB, 1 GB, 0.5 GB of RAM, respectively. In addition, it should be noted that the available memory on the Jetson Nano, Raspberry Pi 3B+, and Pi Zero 2 during idle time is about 1.7 GB, 600 MB, and 250 MB. This is because some of the memory is already being used by background processes, concurrent apps, and the operating system. Hence, we allocate an additional 1GB of swap space, enabling the execution of memory-intensive Meta-CL methods such as ANML+AIM and OML+AIM. Our software stack includes Faiss [Johnson *et al.*, 2019] and PyTorch 1.13 for meta-training and meta-testing stages.

3.6 Experimental Setup

Training Detail: We adopt a pre-training procedure, similar to prior works [Hu *et al.*, 2022; Yosinski *et al.*, 2014]. For the advanced model architectures such as ViT and YAMNet, there exist pre-trained model weights, thus we utilize them directly similar to [Hu *et al.*, 2022]. Then, for the CNN architecture, we pre-train the CNN model with a sufficient number of epochs (i.e., until the validation loss converges), which is consistent with conventional transfer learning for DNNs [Yosinski *et al.*, 2014]. Consistent with prior meta-training research [Lee *et al.*, 2021; Kwon *et al.*, 2024a], we employed a batch size of 1 for the inner-loop updates and 64 for the outer-loop updates across 20,000 steps to ensure the accuracy of our results. To obtain a meta-trained model with the highest possible validation set accuracy, we tested with various learning rates required for both the inner and outer loops. Consequently, we established the learning rate for the inner loop (α) was set to 0.001, and the learning rate for the outer loop (β) was also set to 0.001 for all datasets. In the meta-testing phase, we assessed ten distinct learning rates for each method and reported the best accuracy. To evaluate the precision of rehearsal-based methods, we experimented with

batch sizes of 8 and 16 and observed a minimal performance difference depending on the batch sizes. We selected a batch size of 8 as it requires less memory than larger batch sizes.

We chose to use ANML with CNN architectures and OML with more advanced models like ViT and YAMNet. Our preliminary tests revealed minimal differences between ANML and OML within the same architecture, with ANML slightly outperforming OML in terms of accuracy. Due to this marginal difference, we focused on ANML for CNNs to streamline the analysis. For more complex architectures like ViT and YAMNet, we opted for OML, as ANML introduces additional computational overhead due to an extra layer. Our study concentrated on the performance of methods within specific architectures rather than comparing ANML and OML across all architectures. This streamlined approach allowed us to present a clearer analysis without redundant testing across combinations.

Evaluation Metrics: Following [Beaulieu *et al.*, 2020], this study focuses on the accuracy of unseen samples across new categories in CL. We measure the end-to-end latency, energy consumption, and peak memory by deploying various Meta-CL methods using *MetaCLBench* on edge devices: Jetson Nano, Raspberry Pi 3B+, Raspberry Pi Zero 2. Specifically, we measure system performance metrics by continually learning all given classes for deployed DNNs on embedded devices. Peak memory includes: (1) model memory for updated weights, (2) optimizer memory for gradients and momentum, (3) activations memory for intermediate outputs during weight updates, and (4) rehearsal samples. To measure end-to-end latency and energy consumption, we account for the time and energy required to: (1) load the model and (2) perform Meta-CL using all available samples (e.g., 30) across all classes (e.g., 30 for CIFAR-100 and 10 for GSCv2). Energy consumption is measured by monitoring the power consumption of the edge device using a YOTINO USB power meter. We derive the energy consumption using the equation (Energy = Power x Time).

4 Results & Findings

This section presents comprehensive evaluation results and findings from *MetaCLBench*. Due to page constraints, we present results from two datasets in the main text, with complete results available in the Appendix.

4.1 Main Results

Previous research [Kwon *et al.*, 2024a; Holla *et al.*, 2020], has shown that OML algorithms achieve lower accuracy than ANML algorithms when using 3-layer CNN architectures. Therefore, we focused our experimental investigation exclusively on ANML for CNN-based evaluations. For advanced models like YAMNet and ViT, we prioritized OML evaluation due to their inherent pre-training components, which eliminate the need for additional pre-training through ANML or the AIM module—additions that neither significantly improve accuracy nor justify their computational cost.

Accuracy. We evaluated the test accuracy of six Meta-CL approaches across five datasets against a baseline model. Oracle models (Oracle ANML for CNN, Oracle OML for YAMNet and ViT) establish the upper accuracy bounds and serve as

Table 1: Performance and computational costs, memory footprint of six representative Meta-CL methods using three network architectures on five datasets of image and audio domains. OOM indicates an out-of-memory issue.

Dataset	Method	CNN			
		Accuracy	Memory	Latency	Energy
Mini ImageNet	Pre-trained	0.258	474.5MB	1,198s	5.5KJ
	ANML	0.327	474.5MB	1,152s	5.3KJ
	ANML+AIM	0.331	1,562 MB	OOM	OOM
	OML+AIM	0.187	1,051 MB	1,434s	6.5KJ
	Raw ANML	0.429	897.1 MB	185.610s	810KJ
	Oracle ANML	0.438	475.0 MB	3.414s	15.7KJ
	LifeLearner	0.433	136.7 MB	1,236s	6.17KJ
Urban Sound8K	Pre-trained	0.182	1,382 MB	302s	1.6KJ
	ANML	0.596	1,382 MB	305s	1.6KJ
	ANML+AIM	0.439	2,593 MB	OOM	OOM
	OML+AIM	0.385	2,648 MB	OOM	OOM
	Raw ANML	0.667	1,456 MB	60,120s	279KJ
	Oracle ANML	0.710	1,384 MB	916s	4.5KJ
	LifeLearner	0.650	496 MB	320s	1.7KJ
ViT					
Dataset	Method	Accuracy	Memory	Latency	Energy
Mini ImageNet	Pre-trained	0.234	336.6 MB	2,056s	11.2KJ
	OML	0.255	336.6 MB	2,203s	11.4KJ
	Raw OML	0.454	1,334 MB	301,456s	1150KJ
	Oracle OML	0.512	337.7 MB	6,301s	31KJ
	Latent OML	0.376	336.6 MB	2,250s	13KJ
YAMNet					
Urban Sound8K	Pre-trained	0.186	39.2 MB	912s	5.4KJ
	OML	0.262	39.2 MB	910s	5.4KJ
	Raw OML	0.595	139.3 MB	120,965s	550KJ
	Oracle OML	0.729	42.4 MB	2,501s	21.1KJ
	Latent OML	0.442	39.2 MB	910s	1.6KJ

backpropagation. Table 1 presents the peak memory usage across various methodologies. First, we found that although AIM enhances accuracy, it increases peak usage due to additional parameters and activation storage requirements during training. The memory demands 1,562 MB for MiniImageNet and 2,648 MB for UrbanSound8K, significantly exceeding the RAM capacity of embedded devices such as the Pi 3B+ and resulting out-of-memory (OOM) problems. Consequently, it becomes challenging to utilize it in edge devices. While OML, ANML, Oracle, Pre-trained, and LifeLearner demonstrate lower memory requirements, Pre-trained and ANML are less accurate. LifeLearner emerges as the optimal solution, requiring only 136-496 MB while maintaining accuracy comparable to Oracle through high compression rates. This efficiency is achieved through latent replay, which reduces activation memory and overall memory footprint, making it particularly suitable for resource-constrained environments. In contrast, advanced architectures like ViT and YAMNet demand greater computational resources due to high-dimensional data processing and additional layer training requirements.

End-to-end Latency & Energy Consumption. Table 1 also presents the operational efficiency of Meta-CL methods implemented on Raspberry Pi 3B+, focusing on end-to-end latency and energy consumption. The end-to-end latency comprises four components: model loading (5%), inference (30%), backpropagation (61%), and data processing overhead (4%). First, we measured the end-to-end latency of CL methods on the Raspberry Pi 3B+ across all classes (30 samples per class). LifeLearner achieved fast end-to-end latency. Oracle exhibited higher training latency due to i.i.d. Training over multiple epochs until it converges. AIM's implementation of attention mechanism selection during backpropagation increased computational overhead. LifeLearner reduces training and memory latency through latent replay and model freezing. Due to the large amount of memory required by the AIM series, crashes occurred several times during the test due to memory exhaustion.

To establish generalizability, we extended our evaluation to diverse edge devices with varying computational capabilities (Jetson Nano with enhanced specifications and Pi Zero 2 with reduced capacity). The table 2 below shows the end-to-end latency and energy consumption results across these three edge devices, confirming that LifeLearner achieves a 7.5-fold reduction in latency compared to Oracle.

4.2 Analysis and Discussion

Effectiveness of Pre-training. We examine the effectiveness of pre-training on the performance of Meta-CL methods. Our evaluation across five datasets without pre-training reveals varying performance levels: while the two image datasets and GSCv2 demonstrated satisfactory accuracy, Urbansound and ESC50 showed suboptimal performance. Following the approach used in advanced models, we implemented pre-training before meta-training for each method. As shown in Figure 3a, the incorporation of pre-training significantly enhanced model performance. Notably, Meta-CL methods achieved an average performance improvement of 13.98% on the Urbansound and ESC50 datasets after pre-training. Our analysis revealed that CNNs exhibited considerable performance degradation

benchmarks, as they are trained on all classes simultaneously in an i.i.d. manner, following traditional offline DNN training. By comparing Meta-CL methods against Oracle models, we demonstrate the trade-offs between Meta-CL approaches and ideal scenarios where all data is available initially, highlighting our methods' efficiency under practical constraints. The results in Table 1 show that models using only pre-trained weights ("Pre-trained") achieve lower accuracy, averaging 22.18% and 13.8% across the datasets for Convolutional Neural Networks (CNNs) and advanced architectures(YAMNet and ViT). This result indicates that traditional transfer learning fails to address few-shot learning challenges. In CNN architecture, baseline ANML improved upon the pre-trained-only approach with a 16.7% average accuracy gain. The AIM enhancement further increased accuracy by 2.54%. However, these improvements remained below Oracle and LifeLearner methods by 15.92%. The constrained sample size during the meta-testing phase poses a challenge to attaining high accuracy, even considering the theoretical upper limit.

Peak Memory Footprint. We conducted measurements to ascertain the maximum RAM requirements for backpropagation execution and rehearsal samples storage. The backpropagation memory is divided into three parts: (1) model memory, which is responsible for storing model parameters; (2) optimizer memory, which is responsible for storing gradient and momentum vectors; (3) activation memory, which is responsible for storing intermediate activations that are reused during

Table 2: End-to-end latency and energy consumption results of running different Meta-CL methods on three different edge devices

Device	Method	Latency	Energy
Raspberry Pi 3B+	Pretrained	71s	0.32kJ
	ANML	71s	0.32kJ
	Oracle ANML	570s	2.60kJ
	LifeLearner	76s	0.35kJ
Jetson Nano	Pretrained	79s	0.36kJ
	ANML	79s	0.36kJ
	Oracle ANML	633s	2.00kJ
	LifeLearner	84s	0.39kJ
Raspberry Pi Zero 2	Pretrained	74s	0.33kJ
	ANML	75s	0.33kJ
	Oracle ANML	601s	2.64kJ
	LifeLearner	80s	0.35kJ

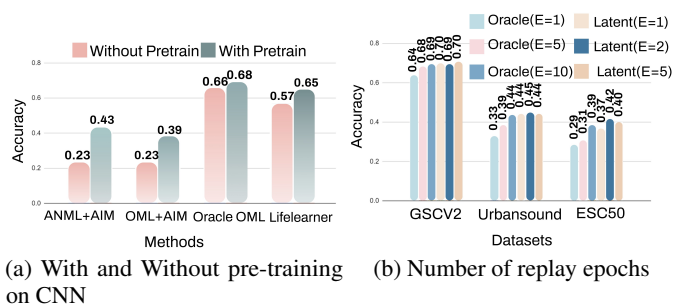


Figure 3: The analysis of Meta-CL Methods for the audio datasets

when meta-training was conducted without pre-training. Given that advanced models inherently contain pre-trained weights, additional pre-training did not yield substantial accuracy improvements. These findings establish pre-training as a crucial step in optimizing model accuracy and demonstrate that the sequential implementation of pre-training followed by meta-training is essential for achieving superior performance across all methods.

The Number of Replay Epochs. We investigated the relationship between replay frequency and accuracy, acknowledging that increased replays correspond to higher latency and energy consumption. As illustrated in Figure 3b, Oracle OML requires more than five replays to achieve high accuracy levels, resulting in increased energy consumption during training. In contrast, Latent OML demonstrates superior efficiency, achieving comparable accuracy with only one or two replays, thus reducing system overhead. Within the same dataset, Latent OML’s performance after five replays approximates that of Oracle OML after ten replays.

Multi Compression Module. In CNN architectures, ANML with AIM demonstrates substantial accuracy improvements (from 26.0% to 34.6% on CIFAR100), albeit at the cost of increased memory requirements (from 39.69MB to 1,093MB). LifeLearner presents an optimal balance between accuracy and memory utilization in resource-constrained environments. The integration of AIM, while beneficial for accuracy, introduces significant computational overhead, par-

ticularly in Raw ANML implementations (11,424s latency, 52.5KJ energy consumption on CIFAR100). Oracle ANML provides a balanced compromise between performance enhancement and resource efficiency.

Vision Transformer (ViT) and YAMNet architectures exhibit analogous performance-resource tradeoffs. ViT implementations with OML and AIM show improved accuracy but incur substantial computational costs (22,968s latency, 103KJ energy consumption on CIFAR100). Similarly, YAMNet with AIM achieves superior accuracy (from 42.9% to 71.0% on GSCv2) while requiring increased memory utilization (from 10.16MB to 608.2MB). Pretrained YAMNet models demonstrate superior resource efficiency metrics.

5 Practical Guidelines

Our extensive empirical analysis provides evidence-based guidelines for researchers and practitioners implementing Meta-CL on edge devices. Although this investigation focuses on specific Meta-CL methods and may not encompass all learning approaches, our results and findings show consistent patterns across different architectures and datasets, which lead to the following key guidelines.

Resource-Aware Method Selection. The choice of Meta-CL implementation should be guided by available system resources. For systems with adequate storage capacity, LifeLearner or Latent OML implementations provide optimal accuracy across datasets. Resource-constrained environments benefit from Raw ANML or Raw OML methods combined with hardware-friendly optimizations. In severely limited environments, efficient integration of the quantization and compression module of LifeLearner with advanced models (YAMNet and ViT) would offer a viable compromise between computational efficiency and storage requirements.

Edge Deployment Considerations. Latent methods consistently demonstrate superior performance across image and audio datasets, balancing accuracy with resource efficiency. This characteristic positions these methods as particularly advantageous for IoT applications, facilitating real-time category integration, efficient personalized processing, and privacy-preserving local computation without additional communication overhead.

6 Conclusion

In this paper, we investigate how to solve the CF problem based on five representative image and audio datasets (i.e., CIFAR100, MiniImageNet, GSCV2, UrbanSound8K, and ESC50) using three different network architectures with different complexities using six well-known Meta-CL methods. We also created a comprehensive Meta-CL benchmark framework on an edge device to assess the system overheads occurring on the device and examine the trade-offs between performance, computational costs, memory usage, and storage of different Meta-CL approaches. We first found that the combination of pre-training plus meta-training plus evaluation maximizes performance. Advanced methods (YAMNet and ViT) already include pre-trained, so the extra pre-training will not affect the results much.

References

- [Ahn *et al.*, 2019] Hongjoon Ahn, Sungmin Cha, Donggyu Lee, and Taesup Moon. Uncertainty-based continual learning with adaptive regularization. *Advances in neural information processing systems*, 32, 2019.
- [Arik *et al.*, 2018] Sercan Arik, Jitong Chen, Kainan Peng, Wei Ping, and Yanqi Zhou. Neural voice cloning with a few samples. *Advances in neural information processing systems*, 31, 2018.
- [Beaulieu *et al.*, 2020] Shawn Beaulieu, Lapo Frati, Thomas Miconi, Joel Lehman, Kenneth O Stanley, Jeff Clune, and Nick Cheney. Learning to continually learn. *arXiv preprint arXiv:2002.09571*, 2020.
- [Chaudhry *et al.*, 2019] Arslan Chaudhry, Marcus Rohrbach, Mohamed Elhoseiny, Thalaiyasingam Ajanthan, P Dokania, P Torr, and M Ranzato. Continual learning with tiny episodic memories. In *Workshop on Multi-Task and Lifelong Reinforcement Learning*, 2019.
- [Chauhan *et al.*, 2020] Jagmohan Chauhan, Young D Kwon, Pan Hui, and Cecilia Mascolo. Contauth: Continual learning framework for behavioral-based user authentication. *Proceedings of the ACM on Interactive, Mobile, Wearable and Ubiquitous Technologies*, 4(4):1–23, 2020.
- [Chauhan *et al.*, 2022] Jagmohan Chauhan, Young D Kwon, and Cecilia Mascolo. Exploring on-device learning using few shots for audio classification. In *2022 30th European Signal Processing Conference (EUSIPCO)*, pages 424–428. IEEE, 2022.
- [Chen *et al.*, 2022] Ke Chen, Xingjian Du, Bilei Zhu, Zejun Ma, Taylor Berg-Kirkpatrick, and Shlomo Dubnov. Hts-at: A hierarchical token-semantic audio transformer for sound classification and detection. In *ICASSP 2022-2022 IEEE International Conference on Acoustics, Speech and Signal Processing (ICASSP)*, pages 646–650. IEEE, 2022.
- [Cheraghian *et al.*, 2021] Ali Cheraghian, Shafin Rahman, Pengfei Fang, Soumava Kumar Roy, Lars Petersson, and Mehrtash Harandi. Semantic-aware knowledge distillation for few-shot class-incremental learning. In *Proceedings of the IEEE/CVF conference on computer vision and pattern recognition*, pages 2534–2543, 2021.
- [Dosovitskiy *et al.*, 2020] Alexey Dosovitskiy, Lucas Beyer, Alexander Kolesnikov, Dirk Weissenborn, Xiaohua Zhai, Thomas Unterthiner, Mostafa Dehghani, Matthias Minderer, Georg Heigold, Sylvain Gelly, et al. An image is worth 16x16 words: Transformers for image recognition at scale. *arXiv preprint arXiv:2010.11929*, 2020.
- [Douillard *et al.*, 2020] Arthur Douillard, Matthieu Cord, Charles Ollion, Thomas Robert, and Eduardo Valle. Podnet: Pooled outputs distillation for small-tasks incremental learning. In *Computer vision–ECCV 2020: 16th European conference, Glasgow, UK, August 23–28, 2020, proceedings, part XX 16*, pages 86–102. Springer, 2020.
- [Fernando *et al.*, 2017] Chrisantha Fernando, Dylan Banarse, Charles Blundell, Yori Zwols, David Ha, Andrei A Rusu, Alexander Pritzel, and Daan Wierstra. Pathnet: Evolution channels gradient descent in super neural networks. *arXiv preprint arXiv:1701.08734*, 2017.
- [Finn *et al.*, 2017] Chelsea Finn, Pieter Abbeel, and Sergey Levine. Model-agnostic meta-learning for fast adaptation of deep networks. In *International conference on machine learning*, pages 1126–1135. PMLR, 2017.
- [Fritzke, 1994] Bernd Fritzke. A growing neural gas network learns topologies. *Advances in neural information processing systems*, 7, 1994.
- [He and Zhu, 2021] Jiangpeng He and Fengqing Zhu. Online continual learning for visual food classification. In *Proceedings of the IEEE/CVF international conference on computer vision*, pages 2337–2346, 2021.
- [Hersche *et al.*, 2022] Michael Hersche, Geethan Karunaratne, Giovanni Cherubini, Luca Benini, Abu Sebastian, and Abbas Rahimi. Constrained few-shot class-incremental learning. In *Proceedings of the IEEE/CVF Conference on Computer Vision and Pattern Recognition*, pages 9057–9067, 2022.
- [Holla *et al.*, 2020] Nithin Holla, Pushkar Mishra, Helen Yannakoudakis, and Ekaterina Shutova. Meta-learning with sparse experience replay for lifelong language learning. *arXiv preprint arXiv:2009.04891*, 2020.
- [Hospedales *et al.*, 2021] Timothy Hospedales, Antreas Antoniou, Paul Micaelli, and Amos Storkey. Meta-learning in neural networks: A survey. *IEEE transactions on pattern analysis and machine intelligence*, 44(9):5149–5169, 2021.
- [Hou *et al.*, 2019] Saihui Hou, Xinyu Pan, Chen Change Loy, Zilei Wang, and Dahua Lin. Learning a unified classifier incrementally via rebalancing. In *Proceedings of the IEEE/CVF conference on computer vision and pattern recognition*, pages 831–839, 2019.
- [Howard *et al.*, 2017] Andrew G Howard, Menglong Zhu, Bo Chen, Dmitry Kalenichenko, Weijun Wang, Tobias Weyand, Marco Andreetto, and Hartwig Adam. Mobilenets: Efficient convolutional neural networks for mobile vision applications. *arXiv preprint arXiv:1704.04861*, 2017.
- [Hu *et al.*, 2022] Shell Xu Hu, Da Li, Jan Stühmer, Minyoung Kim, and Timothy M Hospedales. Pushing the limits of simple pipelines for few-shot learning: External data and fine-tuning make a difference. In *Proceedings of the IEEE/CVF Conference on Computer Vision and Pattern Recognition*, pages 9068–9077, 2022.
- [Hung *et al.*, 2019] Ching-Yi Hung, Cheng-Hao Tu, Cheng-En Wu, Chien-Hung Chen, Yi-Ming Chan, and Chu-Song Chen. Compacting, picking and growing for unforgetting continual learning. *Advances in neural information processing systems*, 32, 2019.
- [Jacob *et al.*, 2018] Benoit Jacob, Skirmantas Kligys, Bo Chen, Menglong Zhu, Matthew Tang, Andrew Howard, Hartwig Adam, and Dmitry Kalenichenko. Quantization and training of neural networks for efficient integer-arithmetic-only inference. In *Proceedings of the IEEE Conference on Computer Vision and Pattern Recognition (CVPR)*, June 2018.

- 776 [Javed and White, 2019] Khurram Javed and Martha White.
 777 Meta-learning representations for continual learning. *Advances in neural information processing systems*, 32, 2019.
 778
- 779 [Jerfel *et al.*, 2019] Ghassen Jerfel, Erin Grant, Tom Griffiths,
 780 and Katherine A Heller. Reconciling meta-learning and
 781 continual learning with online mixtures of tasks. *Advances in neural information processing systems*, 32, 2019.
 782
- 783 [Jha *et al.*, 2021] Saurav Jha, Martin Schiemer, Franco Zam-
 784 bonelli, and Juan Ye. Continual learning in sensor-based
 785 human activity recognition: An empirical benchmark anal-
 786 ysis. *Information Sciences*, 575:1–21, October 2021.
 787
- 788 [Johnson *et al.*, 2019] Jeff Johnson, Matthijs Douze, and
 789 Hervé Jégou. Billion-scale similarity search with GPUs.
IEEE Transactions on Big Data, pages 1–1, 2019.
 790
- 791 [Keshari *et al.*, 2018] Rohit Keshari, Mayank Vatsa, Richa
 792 Singh, and Afzel Noore. Learning structure and strength of
 793 cnn filters for small sample size training. In *proceedings of the IEEE conference on computer vision and pattern*
 794 *recognition*, pages 9349–9358, 2018.
 795
- 796 [Kirkpatrick *et al.*, 2017] James Kirkpatrick, Razvan Pas-
 797 canu, Neil Rabinowitz, Joel Veness, Guillaume Desjardins,
 798 Andrei A Rusu, Kieran Milan, John Quan, Tiago Ramalho,
 799 Agnieszka Grabska-Barwinska, et al. Overcoming catas-
 800 trophic forgetting in neural networks. *Proceedings of the national academy of sciences*, 114(13):3521–3526, 2017.
 801
- 802 [Kozerawski and Turk, 2018] Jedrzej Kozerawski and
 803 Matthew Turk. Clear: Cumulative learning for one-shot
 804 one-class image recognition. In *Proceedings of the IEEE Conference on Computer Vision and Pattern Recognition*,
 805 pages 3446–3455, 2018.
 806
- 807 [Krizhevsky *et al.*, 2009] Alex Krizhevsky, Geoffrey Hinton,
 808 et al. Learning multiple layers of features from tiny images.
 809 2009.
 810
- 811 [Kwon *et al.*, 2021a] Young D Kwon, Jagmohan Chauhan,
 812 Abhishek Kumar, Pan Hui, and Cecilia Mascolo. Explor-
 813 ing System Performance of Continual Learning for Mobile
 814 and Embedded Sensing Applications. In *ACM/IEEE Sym-posium on Edge Computing*. Association for Computing
 815 Machinery (ACM), 2021.
 816
- 817 [Kwon *et al.*, 2021b] Young D. Kwon, Jagmohan Chauhan,
 818 and Cecilia Mascolo. FastICARL: Fast Incremental Clas-
 819 sifier and Representation Learning with Efficient Budget
 Allocation in Audio Sensing Applications. In *Proc. Inter-speech 2021*, pages 356–360, 2021.
 820
- 821 [Kwon *et al.*, 2024a] Young D. Kwon, Jagmohan Chauhan,
 822 Hong Jia, Stylianos I. Venieris, and Cecilia Mascolo. Life-
 823 Learner: Hardware-Aware Meta Continual Learning Sys-
 824 tem for Embedded Computing Platforms. In *Proceedings of the 21st ACM Conference on Embedded Networked Sensor*
 825 *Systems*, SenSys ’23, page 138–151, New York, NY, USA,
 826 2024. Association for Computing Machinery.
 827
- 828 [Kwon *et al.*, 2024b] Young D. Kwon, Rui Li, Stylianos Ve-
 829 nieris, Jagmohan Chauhan, Nicholas Donald Lane, and Ce-
 830 cilia Mascolo. TinyTrain: Resource-Aware Task-Adaptive
 831
- 832 Sparse Training of DNNs at the Data-Scarce Edge. In *Pro-
 833 ceedings of the 41st International Conference on Machine*
 834 *Learning*, volume 235 of *Proceedings of Machine Learning*
 835 *Research*, pages 25812–25843. PMLR, 21–27 Jul 2024.
 836
- 837 [Lake *et al.*, 2015] Brenden M Lake, Ruslan Salakhutdinov,
 838 and Joshua B Tenenbaum. Human-level concept learn-
 839 ing through probabilistic program induction. *Science*,
 840 350(6266):1332–1338, 2015.
 841
- 842 [Lee *et al.*, 2021] Eugene Lee, Cheng-Han Huang, and Chen-
 843 Yi Lee. Few-shot and continual learning with attentive
 844 independent mechanisms. In *Proceedings of the IEEE/CVF*
 845 *international conference on computer vision*, pages 9455–
 846 9464, 2021.
 847
- 848 [Li and Hoiem, 2017] Zhizhong Li and Derek Hoiem. Learn-
 849 ing without forgetting. *IEEE transactions on pattern analy-
 850 sis and machine intelligence*, 40(12):2935–2947, 2017.
 851
- 852 [Li and Hoiem, 2018] Zhizhong Li and Derek Hoiem. Learn-
 853 ing without forgetting. *IEEE Transactions on Pattern Anal-
 854 ysis and Machine Intelligence*, 40(12):2935–2947, 2018.
 855
- 856 [Lin *et al.*, 2022] Ji Lin, Ligeng Zhu, Wei-Ming Chen, Wei-
 857 Chen Wang, Chuang Gan, and Song Han. On-device train-
 858 ing under 256kb memory. *Advances in Neural Information*
 859 *Processing Systems*, 35:22941–22954, 2022.
 860
- 861 [Mai *et al.*, 2022] Zheda Mai, Ruiwen Li, Jihwan Jeong,
 862 David Quispe, Hyunwoo Kim, and Scott Sanner. Online
 863 continual learning in image classification: An empirical
 864 survey. *Neurocomputing*, 469:28–51, 2022.
 865
- 866 [Mallya and Lazebnik, 2018] Arun Mallya and Svetlana
 867 Lazebnik. Packnet: Adding multiple tasks to a single net-
 868 work by iterative pruning. In *Proceedings of the IEEE*
 869 *conference on Computer Vision and Pattern Recognition*,
 870 pages 7765–7773, 2018.
 871
- 872 [Marco *et al.*, 2024] N. Di Marco, Edoardo Loru, Anita
 873 Bonetti, Alessandra Olga Grazia Serra, Matteo Cinelli, and
 874 Walter Quattrociocchi. Patterns of linguistic simplifica-
 875 tion on social media platforms over time. *Proceedings of*
 876 *the National Academy of Sciences*, 121(50):e2412105121,
 877 2024.
 878
- 879 [McCloskey and Cohen, 1989] Michael McCloskey and
 880 Neal J. Cohen. Catastrophic interference in connectionist
 881 networks: The sequential learning problem. volume 24 of
 882 *Psychology of Learning and Motivation*, pages 109–165.
 883 Academic Press, 1989.
 884
- 885 [Michieli *et al.*, 2023] Umberto Michieli, Pablo Peso Parada,
 886 and Mete Ozay. Online Continual Learning in Keyword
 887 Spotting for Low-Resource Devices via Pooling High-
 888 Order Temporal Statistics. In *Proc. INTERSPEECH 2023*,
 889 pages 1628–1632, 2023.
 890
- 891 [Parisi *et al.*, 2019] German I Parisi, Ronald Kemker, Jose L
 892 Part, Christopher Kanan, and Stefan Wermter. Continual
 893 lifelong learning with neural networks: A review. *Neural*
 894 *networks*, 113:54–71, 2019.
 895
- 896 [Paszke *et al.*, 2019] Adam Paszke, Sam Gross, Francisco
 897 Massa, Adam Lerer, James Bradbury, Gregory Chanan,
 898 Trevor Killeen, Zeming Lin, Natalia Gimelshein, Luca
 899

- 885 Antiga, Alban Desmaison, Andreas Kopf, Edward Yang,
 886 Zachary DeVito, Martin Raison, Alykhan Tejani, Sasank
 887 Chilamkurthy, Benoit Steiner, Lu Fang, Junjie Bai, and
 888 Soumith Chintala. Pytorch: An imperative style, high-
 889 performance deep learning library. In *Advances in Neural
 890 Information Processing Systems (NeurIPS)*, 2019.
 891 [Pellegrini *et al.*, 2020] Lorenzo Pellegrini, Gabriele Graffi-
 892 eti, Vincenzo Lomonaco, and Davide Maltoni. Latent re-
 893 play for real-time continual learning. In *2020 IEEE/RSJ
 894 International Conference on Intelligent Robots and Systems
 895 (IROS)*, pages 10203–10209. IEEE, 2020.
 896 [Piczak, 2015] Karol J Piczak. Esc: Dataset for environmen-
 897 tal sound classification. In *Proceedings of the 23rd ACM
 898 international conference on Multimedia*, pages 1015–1018,
 899 2015.
 900 [Pons *et al.*, 2019] Jordi Pons, Joan Serrà, and Xavier Serra.
 901 Training neural audio classifiers with few data. In *ICASSP
 902 2019-2019 IEEE International Conference on Acoustics,
 903 Speech and Signal Processing (ICASSP)*, pages 16–20.
 904 IEEE, 2019.
 905 [Purwins *et al.*, 2019] Hendrik Purwins, Bo Li, Tuomas Vir-
 906 tanen, Jan Schlüter, Shuo-Yiin Chang, and Tara Sainath.
 907 Deep Learning for Audio Signal Processing. *IEEE Journal
 908 of Selected Topics in Signal Processing*, 13(2):206–219,
 909 May 2019.
 910 [Rannen *et al.*, 2017] Amal Rannen, Rahaf Aljundi,
 911 Matthew B. Blaschko, and Tinne Tuytelaars. Encoder
 912 based lifelong learning. In *Proceedings of the IEEE
 913 International Conference on Computer Vision (ICCV)*, Oct
 914 2017.
 915 [Rebuffi *et al.*, 2017] Sylvestre-Alvise Rebuffi, Alexander
 916 Kolesnikov, Georg Sperl, and Christoph H Lampert. icarl:
 917 Incremental classifier and representation learning. In *Pro-
 918 ceedings of the IEEE conference on Computer Vision and
 919 Pattern Recognition*, pages 2001–2010, 2017.
 920 [Rodríguez *et al.*, 2021] Sandra Servia Rodríguez, Cecilia
 921 Mascolo, and Young D. Kwon. Knowing when we do
 922 not know: Bayesian continual learning for sensing-based
 923 analysis tasks. *CoRR*, abs/2106.05872, 2021.
 924 [Rolnick *et al.*, 2019] David Rolnick, Arun Ahuja, Jonathan
 925 Schwarz, Timothy Lillicrap, and Gregory Wayne. Experi-
 926 ence replay for continual learning. *Advances in Neural
 927 Information Processing Systems*, 32, 2019.
 928 [Rusu *et al.*, 2016] Andrei A Rusu, Neil C Rabinowitz, Guil-
 929 laume Desjardins, Hubert Soyer, James Kirkpatrick, Koray
 930 Kavukcuoglu, Razvan Pascanu, and Raia Hadsell. Progres-
 931 sive neural networks. *arXiv preprint arXiv:1606.04671*,
 932 2016.
 933 [Rusu *et al.*, 2018] Andrei A Rusu, Dushyant Rao, Jakub Syg-
 934 nowski, Oriol Vinyals, Razvan Pascanu, Simon Osindero,
 935 and Raia Hadsell. Meta-learning with latent embedding
 936 optimization. *arXiv preprint arXiv:1807.05960*, 2018.
 937 [Salamon *et al.*, 2014] Justin Salamon, Christopher Jacoby,
 938 and Juan Pablo Bello. A dataset and taxonomy for urban
 939 sound research. In *Proceedings of the 22nd ACM interna-
 940 tional conference on Multimedia*, pages 1041–1044, 2014.
 941 [Schwartz *et al.*, 2018] Eli Schwartz, Leonid Karlinsky,
 942 Joseph Shtok, Sivan Harary, Mattias Marder, Abhishek
 943 Kumar, Rogerio Feris, Raja Giryes, and Alex Bronstein.
 944 Delta-encoder: an effective sample synthesis method for
 945 few-shot object recognition. *Advances in neural informa-
 946 tion processing systems*, 31, 2018.
 947 [Shen *et al.*, 2019] Wei Shen, Ziqiang Shi, and Jun Sun.
 948 Learning from adversarial features for few-shot classifi-
 949 cation. *arXiv preprint arXiv:1903.10225*, 2019.
 950 [Shi *et al.*, 2021] Guangyuan Shi, Jiaxin Chen, Wenlong
 951 Zhang, Li-Ming Zhan, and Xiao-Ming Wu. Overcoming
 952 catastrophic forgetting in incremental few-shot learning
 953 by finding flat minima. *Advances in neural information
 954 processing systems*, 34:6747–6761, 2021.
 955 [Shin *et al.*, 2017] Hanul Shin, Jung Kwon Lee, Jaehong Kim,
 956 and Jiwon Kim. Continual learning with deep generative
 957 replay. *Advances in neural information processing systems*,
 958 30, 2017.
 959 [Song *et al.*, 2000] Sen Song, Kenneth D Miller, and Larry F
 960 Abbott. Competitive hebbian learning through spike-
 961 timing-dependent synaptic plasticity. *Nature neuroscience*,
 962 3(9):919–926, 2000.
 963 [Su *et al.*, 2019] Yu Su, Ke Zhang, Jingyu Wang, and Kurosh
 964 Madani. Environment sound classification using a two-
 965 stream cnn based on decision-level fusion. *Sensors*,
 966 19(7):1733, 2019.
 967 [Sun *et al.*, 2019] Qianru Sun, Yaoyao Liu, Tat-Seng Chua,
 968 and Bernt Schiele. Meta-transfer learning for few-shot
 969 learning. In *Proceedings of the IEEE/CVF conference on
 970 computer vision and pattern recognition*, pages 403–412,
 971 2019.
 972 [Tao *et al.*, 2020] Xiaoyu Tao, Xinyuan Chang, Xiaopeng
 973 Hong, Xing Wei, and Yihong Gong. Topology-preserving
 974 class-incremental learning. In *Computer Vision–ECCV
 975 2020: 16th European Conference, Glasgow, UK, August
 976 23–28, 2020, Proceedings, Part XIX 16*, pages 254–270.
 977 Springer, 2020.
 978 [Thusseethan *et al.*, 2021] Selvarajah Thusseethan, Sutharshan
 979 Rajasegarar, and John Yearwood. Deep continual learning
 980 for emerging emotion recognition. *IEEE Transactions on
 981 Multimedia*, 24:4367–4380, 2021.
 982 [Vinyals *et al.*, 2016] Oriol Vinyals, Charles Blundell, Tim-
 983 othy Lillicrap, Daan Wierstra, et al. Matching networks
 984 for one shot learning. *Advances in neural information
 985 processing systems*, 29, 2016.
 986 [Wang *et al.*, 2020] Yaqing Wang, Quanming Yao, James T
 987 Kwok, and Lionel M Ni. Generalizing from a few examples:
 988 A survey on few-shot learning. *ACM computing surveys
 989 (csur)*, 53(3):1–34, 2020.
 990 [Wang *et al.*, 2024] Liyuan Wang, Xingxing Zhang, Hang Su,
 991 and Jun Zhu. A Comprehensive Survey of Continual Learn-
 992 ing: Theory, Method and Application. *IEEE Transactions
 993 on Pattern Analysis and Machine Intelligence*, 46(8):5362–
 994 5383, 2024.

- 995 [Warden, 2018] Pete Warden. Speech commands: A dataset
996 for limited-vocabulary speech recognition. *arXiv preprint*
997 *arXiv:1804.03209*, 2018.
- 998 [Wu *et al.*, 2019] Yue Wu, Yinpeng Chen, Lijuan Wang,
999 Yuancheng Ye, Zicheng Liu, Yandong Guo, and Yun Fu.
1000 Large scale incremental learning. In *Proceedings of the*
1001 *IEEE/CVF conference on computer vision and pattern*
1002 *recognition*, pages 374–382, 2019.
- 1003 [Yoo *et al.*, 2018] Donghyun Yoo, Haoqi Fan, Vishnu Bod-
1004 deti, and Kris Kitani. Efficient k-shot learning with regular-
1005 ized deep networks. In *Proceedings of the AAAI conference*
1006 *on artificial intelligence*, volume 32, 2018.
- 1007 [Yoon *et al.*, 2017] Jaehong Yoon, Eunho Yang, Jeongtae Lee,
1008 and Sung Ju Hwang. Lifelong learning with dynamically
1009 expandable networks. *arXiv preprint arXiv:1708.01547*,
1010 2017.
- 1011 [Yosinski *et al.*, 2014] Jason Yosinski, Jeff Clune, Yoshua
1012 Bengio, and Hod Lipson. How transferable are features
1013 in deep neural networks? *Advances in neural information*
1014 *processing systems*, 27, 2014.
- 1015 [Zamir, 1998] Ram Zamir. A proof of the fisher information
1016 inequality via a data processing argument. *IEEE Transac-*
1017 *tions on Information Theory*, 44(3):1246–1250, 1998.
- 1018 [Zenke *et al.*, 2017] Friedemann Zenke, Ben Poole, and
1019 Surya Ganguli. Continual learning through synaptic intel-
1020 ligence. In *International conference on machine learning*,
1021 pages 3987–3995. PMLR, 2017.
- 1022 [Zhai *et al.*, 2019] Xiaohua Zhai, Joan Puigcerver, Alexander
1023 Kolesnikov, Pierre Ruyssen, Carlos Riquelme, Mario Lu-
1024 cic, Josip Djolonga, Andre Susano Pinto, Maxim Neumann,
1025 Alexey Dosovitskiy, et al. A large-scale study of represen-
1026 tation learning with the visual task adaptation benchmark.
1027 *arXiv preprint arXiv:1910.04867*, 2019.
- 1028 [Zhang *et al.*, 2020] Junting Zhang, Jie Zhang, Shalini Ghosh,
1029 Dawei Li, Serafettin Tasci, Larry Heck, Heming Zhang, and
1030 C-C Jay Kuo. Class-incremental learning via deep model
1031 consolidation. In *Proceedings of the IEEE/CVF winter*
1032 *conference on applications of computer vision*, pages 1131–
1033 1140, 2020.
- 1034 [Zhang *et al.*, 2021] Chi Zhang, Nan Song, Guosheng Lin,
1035 Yun Zheng, Pan Pan, and Yinghui Xu. Few-shot incre-
1036 mental learning with continually evolved classifiers. In
1037 *Proceedings of the IEEE/CVF conference on computer vi-*
1038 *sion and pattern recognition*, pages 12455–12464, 2021.
- 1039 [Zhou *et al.*, 2022] Da-Wei Zhou, Fu-Yun Wang, Han-Jia Ye,
1040 Liang Ma, Shiliang Pu, and De-Chuan Zhan. Forward
1041 compatible few-shot class-incremental learning. In *Pro-*
1042 *ceedings of the IEEE/CVF conference on computer vision*
1043 *and pattern recognition*, pages 9046–9056, 2022.
- 1044 [Zhu *et al.*, 2021] Kai Zhu, Yang Cao, Wei Zhai, Jie Cheng,
1045 and Zheng-Jun Zha. Self-promoted prototype refinement
1046 for few-shot class-incremental learning. In *Proceedings of*
1047 *the IEEE/CVF conference on computer vision and pattern*
1048 *recognition*, pages 6801–6810, 2021.

Supplementary Material

MetaCLBench: Meta Continual Learning Benchmark on Resource-Constrained Edge Devices

1049

1050
1051

Table of Contents

A	Detailed Benchmark Framework	13
1053	A.1 Additional Baselines & Methods	13
1054	A.2 Datasets	14
1055	A.3 Model Architectures	15
1056	A.4 Detailed Experimental Setup	15
B	Additional Results	16
1058	B.1 Accuracy	16
1059	B.2 Peak Memory Footprint	17
1060	B.3 End-to-end Latency & Energy Consumption	18
C	Further Analysis and Discussion	18
1061	C.1 With and Without pre-training on CNN	18
1062	C.2 Number of replay epochs	18
1063	C.3 Multi Compression Module.	19
D	Extended Related Work	20
1065	D.1 Continual Learning	20
1066	D.2 Meta Learning	21
1067	D.3 Meta Continual Learning	22

1069
1070

A Detailed Benchmark Framework

This section provides additional information on our MetaCLBench framework.

A.1 Additional Baselines & Methods

Pretrained: To initialize the model weights, this baseline performs conventional deep neural network (DNN) training without meta-learning procedure and/or Meta-CL methods during the meta-training phase. After that, it finetunes the model weights with a few samples during a meta-testing phase, similar to other Meta-CL methods. As Pretrained typically shows low performance, it serves as the *lower bound* in our evaluation. Also, a comparison between this baseline and other methods can reveal the effectiveness of the meta-learning procedure in a CL task.

Oracle: This baseline represents the case where it has access to all the classes at once in an i.i.d. fashion. Also, we assume that Oracle would perform DNN training for multiple epochs until the model converges. As a result, Oracle often shows superior accuracy, and thus its accuracy represents the *upper bound* of our evaluation.

OML [Javed and White, 2019]: This method constantly optimizes representations during online updates to quickly acquire predictions for new tasks, facilitating seamless and efficient CL. This approach uses CF as signals to justify the use of storage space to accommodate new tasks. The OML can accomplish CL in more than 200 consecutive classes. It is an online updating method that constantly learns representations and often outperforms rehearsal-based continuous learning methods. The fundamental difference between OML and MAML-Rep lies in their approach to updates. OML employs a single data point for each update, while MAML-Rep utilizes an entire batch. By adopting this method, OML is able to more accurately consider the impact of online learning, including the phenomenon of CF. The objective of OML is to implement the computation graph for live updates and to discover representations that maintain high accuracy even with ongoing changes. It acquires sparse representations without any inactive neurons, surpassing traditional and rehearsal-based strategies for ongoing learning. The technique entails meta-training, with an emphasis on avoiding interference and facilitating rapid adaption during online updates.

ANML [Beaulieu et al., 2020]: This is an approach inspired by the neuromodulation process in the brain. This method accomplishes selective activation (forward pass) and selective plasticity (backward pass) in DNNs by meta-learning through a CL process within the prediction network. Optimizing activation timing by controlling the activation of a predictive model based on input conditions enhances CL. It is often reported to be superior to OML, as it can be optimized to reduce both forward and backward interference. ANML’s architecture comprises two parallel networks: the NM network governs the activations and plasticity of the PLN. ANML employs a unique method where it adjusts specific components of the PLN based on whether it is in the meta-training or meta-testing phase, distinguishing it from conventional methods. The results of the experiments demonstrate that ANML surpasses other approaches by a large margin. It maintains a high level of accuracy even when faced with 600 consecutive tasks. This is attributed to its capability to generate sparse yet powerful representations and effectively manage sequential learning without erasing previously acquired knowledge.

OML+AIM [Lee et al., 2021]: This is a Meta-CL approach that integrates Attentive Independent Mechanisms (AIM), which is a modular component of the OML framework. AIM increases the speed of learning a new task by selecting out the mechanism that best explains the representation of the inner loop to activate. AIM is comprised of a collection of autonomous mechanisms, with each mechanism being defined by its own unique set of parameters. Each mechanism functions as an autonomous specialist that cooperates with other specialists to solve assignments. AIM is situated between the feature extractor and the output classifier in a deep neural network. This approach incorporates higher-level data representation and employs rapidly updated weights within the inner loop of a meta-learning process. During the training process, AIM mechanisms engage in competition and focus on input representations through cross-attention. This allows them to select a limited number of mechanisms for task-specific learning.

ANML+AIM [Lee et al., 2021]: This is a Meta-CL approach that incorporates AIM into the ANML framework. The accuracy of SOTA Meta-CL continues to improve beyond the performance of the previous three approaches by integrating AIM into the existing CL framework. AIM is positioned following a feature extractor and preceding an output classifier, allowing it to effectively process intricate representations. AIM, in contrast to RIMs, does not employ LSTM-based temporal modeling, rendering it a static module. AIM’s processes engage in a targeted manner according to the relevance of the information, which helps to create a concise representation and enhance the ability to adapt to new activities while reducing the risk of CF. It has demonstrated substantial enhancements in accuracy for tasks involving few-shot and ongoing learning, surpassing existing approaches without increasing the number of parameters.

Lifelearner [Kwon et al., 2024a]: This module is based on ANML and combines both lossy and lossless compression to achieve high compression rates and minimize footprint. The Lifelearner approach not only achieves optimal CL efficiency but also significantly reduces energy consumption and latency compared to the SOTA. LifeLearner consists of two distinct phases: meta-training, which takes place on a server to establish a strong initial weight configuration, and meta-testing, which occurs on devices to continuously acquire knowledge of new classes while retaining information from prior ones. The main characteristics consist of an enhanced compression module that minimizes memory consumption, a feature extractor that remains unchanged, and a classifier that is constantly updated through learning. And it achieves efficient learning even on resource-constrained edge devices.

Latent OML: This module is based on OML and incorporates the Compression modular from Lifelearner to achieve high compression rates and minimal footprint. It is used in the testing of advanced architectures (YAMNet and ViT).

1130 A.2 Datasets

1131 To complement the relative simplicity, limited variety, and lack of generalizability of the datasets tested in previous studies, we
1132 added three audio datasets to the single-label image datasets (*CIFAR-100* [Krizhevsky *et al.*, 2009], *MiniImageNet* [Vinyals *et*
1133 *al.*, 2016]) from previous studies. Specifically, we used the *UrbanSound8K* [Salamon *et al.*, 2014] dataset with fewer classes,
1134 the *ESC-50* [Piczak, 2015] dataset with more classes, and the *GSCv2* [Warden, 2018] dataset for keyword spotting (KWS). We
1135 demonstrate trade-offs between performance and system resources on resource-constrained devices by extensively evaluating
1136 these datasets in different Meta-CL approaches. The details of each target dataset employed in our study are described below.

1137 **CIFAR-100** [Krizhevsky *et al.*, 2009]. This dataset, developed by researchers supported by the Canadian Institute for
1138 Advanced Research, has 60,000 photos categorized into 100 classes, with each class including 600 images. The creation of
1139 this used the identical technique as CIFAR-10. The images were obtained by utilizing search phrases from WordNet, and any
1140 duplicate or irrelevant images were eliminated. The dataset is structured into 20 superclasses, with each superclass consisting
1141 of 5 associated classes. The labelers meticulously inspected and assigned labels to each image based on precise instructions,
1142 guaranteeing that each class was distinct from the classes in CIFAR-10. This ensures that CIFAR-100 may be effectively used as
1143 a negative example for CIFAR-10. The dataset is designed for the purpose of training models in object recognition, specifically
1144 focusing on small, natural photos.

1145 **MiniImageNet** [Vinyals *et al.*, 2016]. This dataset was formed by randomly choosing 100 classes from the complete ImageNet
1146 dataset. Each class in the Mini-ImageNet dataset consists of 600 color images, each having dimensions of 84x84 pixels. The
1147 classes were partitioned into 80 for training and 20 for testing, with the guarantee that the test classes were never exposed during
1148 the training process. This dataset is intentionally more intricate than CIFAR-10, but still feasible for contemporary machine
1149 memory. It enables quick development and experimentation. ImageNet is an extensive visual recognition dataset comprising
1150 more than 14 million photos categorized based on the WordNet hierarchy. Every image is annotated with the corresponding thing
1151 it depicts. The dataset facilitates a range of computer vision tasks, such as object detection, classification, and segmentation. For
1152 the purpose of classification, it includes a collection of photos spanning 1,000 different categories. ImageNet's extensive size and
1153 wide range of variations have established it as a standard for training and assessing deep learning models.

1154 **UrbanSound8K** [Salamon *et al.*, 2014]. The development of UrbanSound required the compilation of a wide-ranging and
1155 comprehensive dataset of urban noises. The researchers made use of the Freesound archive, which contains more than 160,000
1156 recordings contributed by users, with a significant number of them being from metropolitan environments. They conducted a
1157 search and retrieved recordings by utilizing specified class names, manually weeding out non-field recordings. The outcome of
1158 this was the acquisition of 1302 recordings, amounting to a total of 27 hours of audio. Out of these, 18.5 hours were dedicated to
1159 manually annotating sound occurrences in 10 different categories, namely air conditioner, car horn, children playing, dog bark,
1160 drilling, engine idling, pistol shot, jackhammer, siren, and street music. Every recording was marked with annotations indicating
1161 the precise start and end times of sound events, as well as their prominence, whether they were in the foreground or background.
1162 UrbanSound8K is a subset of a dataset specifically created to train sound classification algorithms. It contains 8.75 hours of
1163 audio that has been divided into 4-second segments. The taxonomy classifies sounds into four main groups: human, nature,
1164 mechanical, and music, enabling thorough and methodical examination of urban noises.

1165 **ESC-50** [Piczak, 2015]. The primary objective of creating the ESC-50 dataset was to alleviate the limited availability of freely
1166 accessible datasets containing ambient sounds. The dataset comprises 2,000 audio clips, each tagged and lasting 5 seconds. These
1167 clips are categorized into 50 classes, which are further separated into five key categories: animal sounds, natural soundscapes
1168 and water sounds, human non-speech sounds, interior/domestic sounds, and exterior/urban noises. The selection of clips was
1169 carefully picked to prioritize the prominence of sound events while minimizing the presence of background noise. The quality
1170 control process included CrowdFlower's methods and additional validation by the author, resulting in approximately twelve
1171 human categorization entries per clip. The dataset was generated with the purpose of aiding research in the field of environmental
1172 sound categorization, providing a reliable benchmark for the evaluation of automatic sound recognition systems. The dataset is
1173 accessible to the public and contains an additional set of 250,000 video clips without labels, which can be used for unsupervised
1174 learning experiments. The ESC-50 dataset is a valuable resource for investigating machine learning methods in the field of
1175 ambient sound classification.

1176 **GSCv2** [Warden, 2018]. This dataset, created by Pete Warden from Google Brain, seeks to simplify the process of training and
1177 evaluating keyword-detecting systems. The creation of the "Speech Commands" dataset entailed gathering spoken words from a
1178 varied collection of speakers through a web-based application that utilized the WebAudioAPI to record utterances. The dataset
1179 comprises 35 distinct word utterances, encompassing categories such as numbers, frequent instructions, and miscellaneous terms
1180 such as "tree" and "wow". The dataset is specifically intended for limited-vocabulary speech recognition tasks, with the objective
1181 of identifying instances where one of the target words is spoken from a selection of ten or fewer terms. In addition, the dataset
1182 contains recordings of background noise to use in training models to distinguish between speech and non-speech audio. The
1183 objective was to record audio that accurately represented the task of on-device trigger phrases, with a specific emphasis on 10
1184 words: "Yes", "No", "Up", "Down", "Left", "Right", "On", "Off", "Stop", and "Go". Every user would activate a "Record" button,
1185 and a randomly selected word would appear on the screen for a duration of 1.5 seconds while audio was being captured. The
1186 audio snippets were saved as 16-bit single-channel PCM values at a 16 KHz rate in the form of one-second WAV files. The
1187 dataset was specifically curated to be appropriate for training and assessing keyword spotting systems, with an emphasis on
1188 offering a specialized dataset that distinguishes itself from conventional datasets utilized for complete sentence automatic speech

recognition. 1189

A.3 Model Architectures 1190

Referring to previous work [Lin *et al.*, 2022], we add optimized DNN architectures and transformer architectures intended for resource-limited IoT devices to the evaluated three-layer CNN architectures, including **YAMNet** [Howard *et al.*, 2017], and **ViT** [Dosovitskiy *et al.*, 2020]. YAMNet employs the MobileNetV1, which is a highly efficient model specifically designed for applications involving mobile and embedded vision. Depthwise separable convolutions are utilized in their construction, thereby reducing computing complexity by decomposing the normal convolution operation into separate depthwise and pointwise convolutions. This efficient structure enables the development of compact deep neural networks. MobileNets additionally incorporate two hyperparameters, namely width multiplier and resolution multiplier, that allow for adjusting the balance between model size, latency, and accuracy. Developers can tailor MobileNets to match the precise resource limitations of their application by fine-tuning these hyperparameters. MobileNets have demonstrated equivalent performance to larger, more intricate models, but with a substantially smaller size and faster computational speed. They have been effectively utilized in a wide range of activities including item identification, precise categorization, facial features, and other applications. YAMNet provides a flexible and effective approach for implementing deep learning models on mobile and embedded devices. Moreover, MobileNets may be customized to meet unique application needs by modifying the hyperparameters, rendering them adaptable and effective solutions for on-device artificial intelligence. The Vision Transformer (ViT) is an architecture based on transformers, which has demonstrated encouraging outcomes in activities related to image identification. ViT, unlike typical Convolutional Neural Networks (CNNs), operates on inputs in a 2-dimensional format instead of a 1-dimensional series of patches. The model includes Axial Transformer blocks, consisting of row-self-attention followed by a multi-layer perceptron (MLP), and then column-self-attention followed by an MLP, instead of the conventional self-attention followed by an MLP. ViT has undergone pre-training using extensive datasets such as ImageNet-21k and JFT-300M. It has demonstrated exceptional performance on several image recognition benchmarks, including ImageNet, CIFAR-100, and the VTAB classification suite [Zhai *et al.*, 2019], surpassing all previous records. ViT models exhibit superior memory efficiency and outperform CNNs with reduced computational resources. They can be optimized for specific tasks such as detection and segmentation, and demonstrate potential for scenarios with limited data transport. ViT is a transformer-based model that has shown impressive results in image identification tasks, particularly when it is pre-trained on extensive datasets and then fine-tuned for specific applications. 1202
1203
1204
1205
1206
1207
1208
1209
1210
1211
1212
1213
1214

A.4 Detailed Experimental Setup 1215

Training Detail: Consistent with prior meta-training research, we employed a batch size of 1 for the inner-loop updates and 64 for the outer-loop updates across 20,000 steps to ensure the accuracy of our results. To obtain a meta-trained DNN with the highest possible validation set accuracy, we tested with various learning rates required for both the inner and outer loops. Consequently, we established the learning rate for the inner loop (α) was set to 0.001, and the learning rate for the outer loop (β) was also set to 0.001 for all datasets. During the ESC-50 test, we conducted five training sessions, using 1600 clips as the training set and 400 clips as the test set. In the meta-testing phase, we assessed ten distinct learning rates for each technique and reported the most successful outcomes. Additionally, to evaluate the precision of replay systems, we experimented with batch sizes of 8 and 16. We noticed minimal fluctuations in the performance of CL. We selected a batch size of 8 because it requires less memory than larger batch sizes. 1224
1225
1226
1227
1228
1229
1230
1231
1232
1233
1234
1235
1236

Evaluation Protocol: With reference to previous research [Beaulieu *et al.*, 2020], this study prioritizes the accuracy of unseen samples across new categories in CL. The accuracy rate signifies the capacity of CL to make generalizations. In addition, we analytically calculate the memory footprint required to perform CL (model parameters, optimizers, and activations memory). To obtain the peak memory footprint during the CL process, we include (1) model memory for the model itself and the weights to be updated, (2) optimizer memory for gradients, and (3) activations memory for intermediate outputs for weights update. Furthermore, we measure the end-to-end latency and energy consumption of various approaches to CL on the edge device over specified categories. To measure the end-to-end latency and energy, we include the time and energy used to: (1) load a model and (2) perform CL using all the given samples (e.g., 30) over all the given classes (e.g., 10). We test the latency and total energy expenditure for end-to-end CL by deploying MetaCLBench and baselines on an edge device, Raspberry Pi 3B+. Regarding energy, we measure the total amount of energy consumed by a device during the end-to-end CL process. This is performed by measuring the power consumption on Raspberry Pi 3B+ using a YOTINO USB power meter and deriving the energy consumption following the equation: Energy = Power \times Time. 1237
1238
1239
1240

System Implementation: The initial phase of Meta-CL is the meta-training stage, which facilitates swift deployment of the model by initializing the neural network with pre-trained weights. Subsequently, the meta-testing phase incorporates optimizations compatible with hardware, enhancing system efficiency when implemented on embedded devices such as Raspberry Pi 3B+. Source code of MetaCLBench will be publicly available upon publication². 1241
1242
1243
1244

Embedded Device: The Raspberry Pi 3B+ is equipped with a quad-core ARM Cortex-A53 processor and has 1 GB of RAM. It should be noted that the available memory on the Raspberry Pi 3B+ while it is not in use is approximately 600 MB. This is because some of the memory is already being used by background processes, concurrent apps, and the operating system. We 1245
1246
1247
1248

²<https://github.com/theyoungkwon/MetaCLBench>

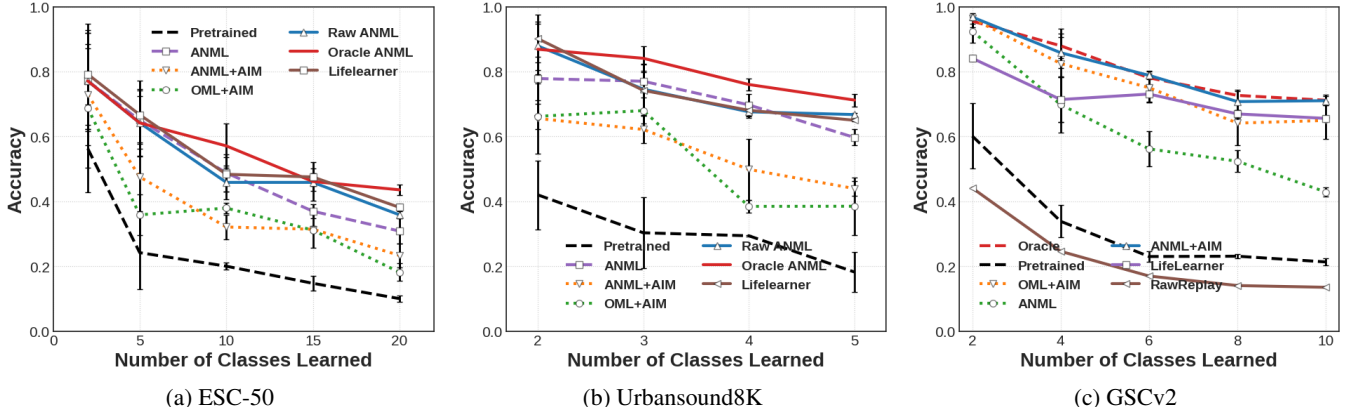


Figure 4: The accuracy of ESC-50, Urbansound8k, GSCv2 datasets using the **3-Layer CNN** architecture.

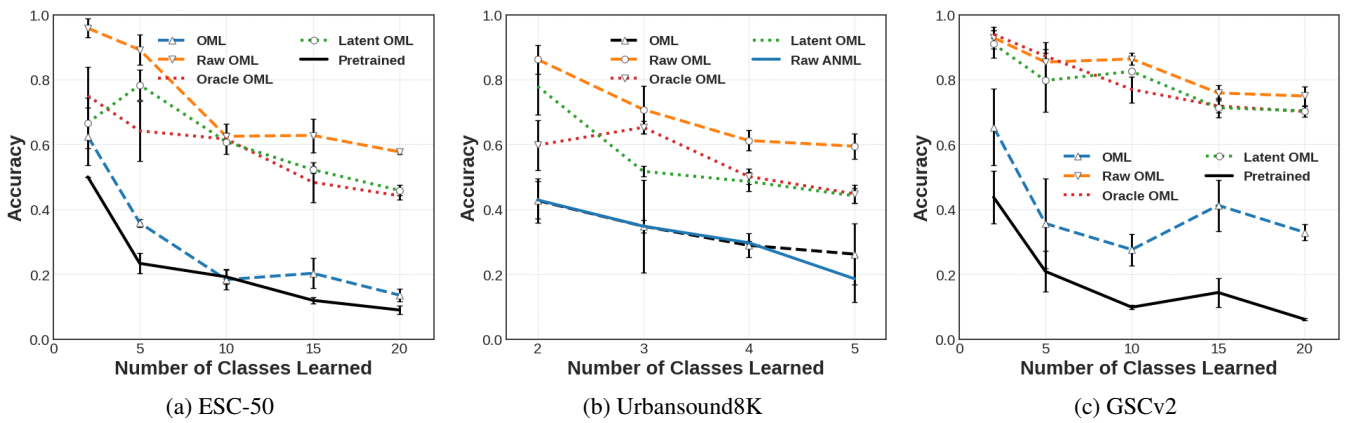


Figure 5: The accuracy of ESC-50, Urbansound8k, GSCv2 datasets using the **YAMNet** architecture.

utilize Faiss (PQ Framework) [Johnson *et al.*, 2019] and PyTorch 1.13 (Deep Learning Framework) [Paszke *et al.*, 2019] as software platforms to create and assess the meta-training and meta-testing stages on embedded devices.

B Additional Results

In this section, we present additional results that are not included in the main content of the paper due to the page limit.

B.1 Accuracy

To visualize the change in accuracy as the training set grows and how each Meta-CL method compares, we provide the results of accuracy on the three architectures (3-layer CNN, YAMNet, and ViT) and six Meta-CL methods based on the five datasets as shown in Figures 4, 5, 6, and 7. The results reveal that models relying solely on pre-trained weights ("Pretrained") exhibit lower accuracy, averaging 22.18% and 13.8% across the datasets for CNNs and more advanced architectures, such as YAMNet and ViT. This result indicates that traditional transfer learning fails to address the complexities of few-shot learning scenarios. Within CNNs, baseline methods like ANML demonstrated improvement over the pretrained-only approach (with an average accuracy gain of 16.7%). This improvement was further augmented by incorporating the AIM, resulting in an additional 2.54% average accuracy gain. However, these gains still fell short of those achieved by the Oracle and Lifelearner methods (by a deficit of 15.92% in accuracy). The constrained sample size in the meta-testing phase poses a challenge to attaining high accuracy levels, even considering the theoretical upper limit of accuracy. Our research also indicated that both CNNs and advanced models experience a marked decline in performance when meta-training proceeds without prior pre-training, noting an average 13.98% improvement after pre-training. Given that advanced models intrinsically include pre-trained weights, further pre-training does not substantially increase their accuracy. Thus, pre-training is affirmed as a critical step for enhancing model accuracy. This study underscores that regardless of the method employed, the procedural sequence of pre-training followed by meta-training before evaluation is indispensable for attaining heightened accuracy levels, recognizing that advanced models inherently incorporate a

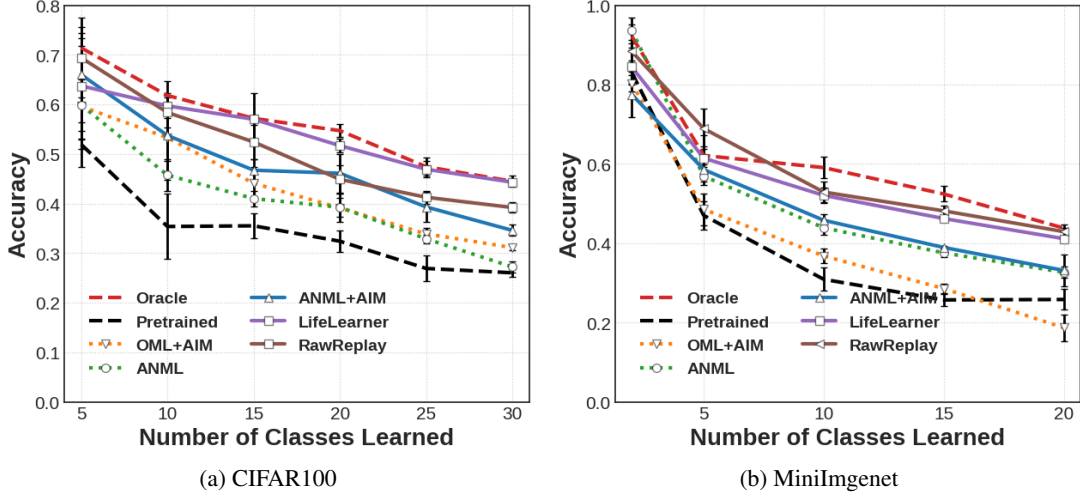


Figure 6: The accuracy of CIFAR100, MiniImagenet datasets using the **3-Layer CNN** architecture.

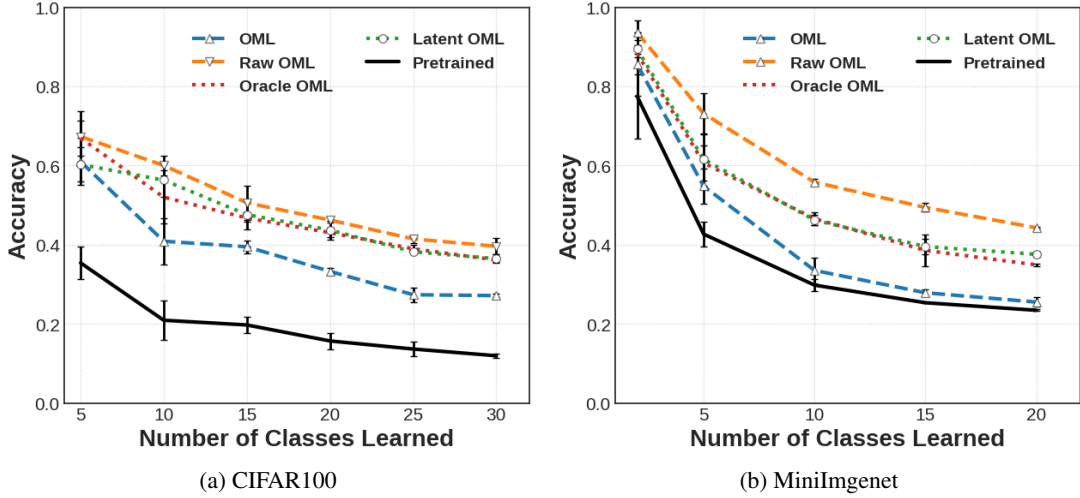


Figure 7: The accuracy of CIFAR100, MiniImagenet datasets using the **ViT** architecture.

pre-training phase. These observations indicate a non-trivial trade-off between accuracy, memory, and computation for all the employed architectures in our work.

B.2 Peak Memory Footprint

Measurements were conducted to ascertain the maximum amount of RAM required for executing backpropagation and storing rehearsal samples. The memory for performing backpropagation is divided into three parts: (1) model memory, which is responsible for storing model parameters; (2) optimizer memory, which is responsible for storing gradient and momentum vectors; (3) activation memory, which is responsible for storing intermediate activations that are reused during backpropagation. Table 3 shows the various methods and the peak memory usage of our system. First, we found that although AIM improves accuracy, it takes up much memory space because there are many parameters in the AIM module. The memory required is as large as 1,562 MB for MiniImageNet and 2,648 MB for UrbanSound8K, which far exceeds the RAM capacity of embedded devices like the Pi 3B+ and causes an out-of-memory (OOM) problem. Consequently, it becomes challenging to utilize it in edge devices. OML, ANML, Oracle, Pretrained, and LifeLearner have a more minor memory requirement. However, Pretrained and ANML are less accurate. In contrast, LifeLearner is the most satisfactory, requiring only 136-496 MB of very high compression rates with high accuracy comparable to Oracle.

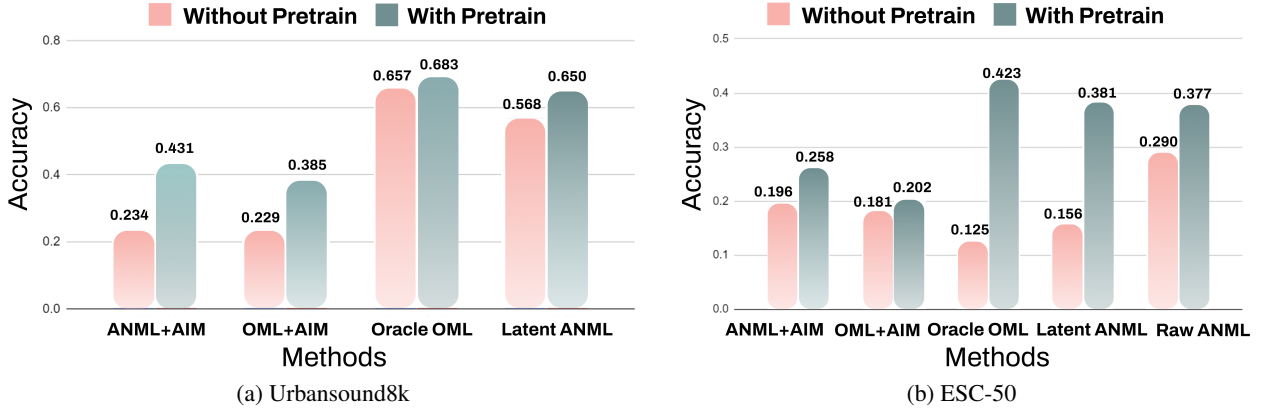


Figure 8: Comparison of accuracy with and without pretraining for datasets UrbanSound8K and ESC-50 using the 3-Layer CNN architecture.

B.3 End-to-end Latency & Energy Consumption

Table 3 also presents the operational efficiency of various Meta-CL methods on edge devices, with specific emphasis on end-to-end latency and energy consumption. The end-to-end latency is calculated by taking into account three different times: (1) The duration required for loading the pre-trained model, (2) The duration needed for sequentially training the model for each specified class, and (3) The duration needed for employing further optimization proposed in specific Meta-CL methods such as compression method of LifeLearner or training additional module such as AIM. First, we measured the end-to-end latency of CL for all systems on the Raspberry Pi CPU for all classes for each dataset (30 samples per class). LifeLearner achieved fast end-to-end latency. Due to the large amount of memory required by the AIM series, crashes occurred several times during the test due to memory exhaustion. While Raw OML may exhibit the highest accuracy among advanced architectures, our tests have demonstrated that Raw methods also require the most computational resources in terms of latency and energy consumption. Additionally, our findings indicate that the YAMNet architecture significantly decreases capacity requirements due to its smaller size; however, it exhibits greater delays and higher energy consumption as a result of its more intricate architecture compared to CNN. As a result, we must consider factors beyond a single result alone when selecting Meta-CL methods for edge devices.

To establish generalizability, we extended our evaluation to diverse edge devices with varying computational capabilities (Jetson Nano with enhanced specifications and Pi Zero 2 with reduced capacity). Table 2 below shows the end-to-end latency and energy consumption results across these three edge devices, confirming that LifeLearner achieves a 7.5-fold reduction in latency compared to Oracle.

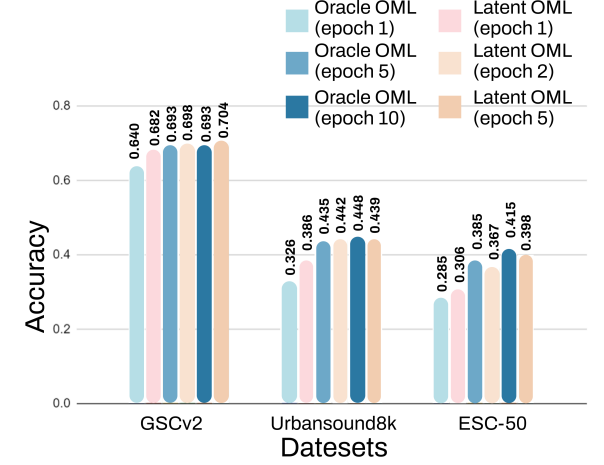
C Further Analysis and Discussion

C.1 With and Without pre-training on CNN

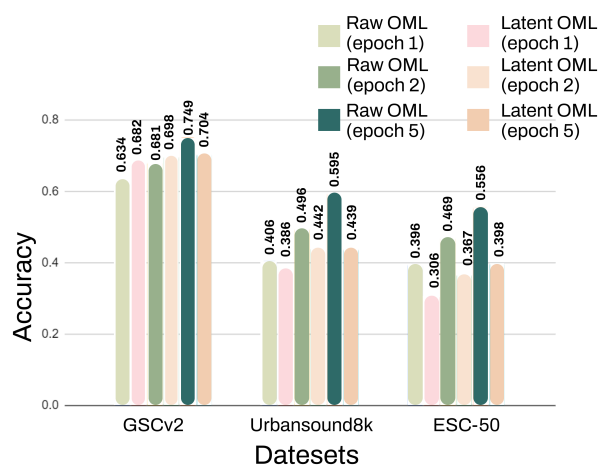
In this section, we examine the impact of hyperparameter variations on model accuracy. First, we investigate the influence of pre-training on the accuracy metric. Initially, we evaluated the five datasets without pre-training; the two image datasets and GSCv2 exhibited satisfactory accuracy. However, the performance on Urbansound8k and ESC-50 was suboptimal. Consequently, we adopted the strategy of pre-training as employed in advanced models, incorporating pre-training before meta-training for each method. Figure 8 illustrates that including pre-training significantly enhances model efficacy. Specifically, in the Urbansound8k and ESC-50 datasets, all Meta-CL methods demonstrated an average efficiency increase of 13.98% following pre-training. Consequently, pre-training plays a significant role in enhancing accuracy, particularly for fundamental algorithms such as ANML and OML, where accuracy without pre-training is a mere 5%. Advanced architectures intrinsically incorporate pre-training, obviating the need for additional pre-processing. Nonetheless, these sophisticated architectures, when incorporating pre-training, exhibit increased latency and energy consumption.

C.2 Number of replay epochs

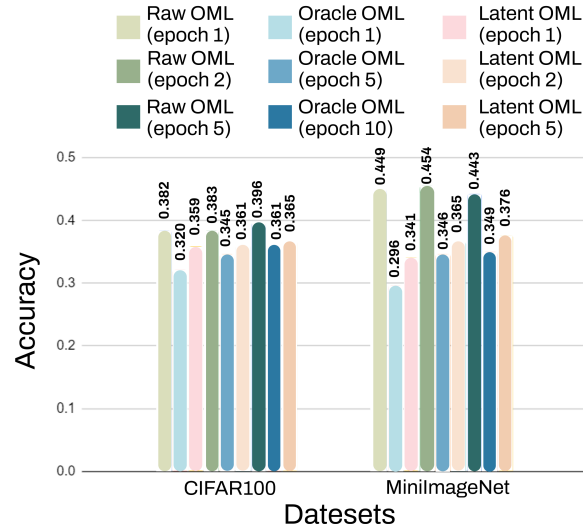
Recognizing that an increased number of replays correlates with heightened latency and energy usage, we explored the association between replay frequency and accuracy. Figure 9a indicates that Oracle OML necessitates more than five replays to attain elevated accuracy levels, thereby escalating energy expenditure throughout the training phase. Conversely, Latent OML demonstrates superior performance, requiring merely one or two replays to reach comparable accuracy, thereby diminishing system overhead. In the case of the same dataset, the efficiency of Latent OML after five replays approximates that of Oracle OML following ten replays. The same observation is evident in the CNN architecture depicted in Figure 9d; here, one or two iterations of the Latent



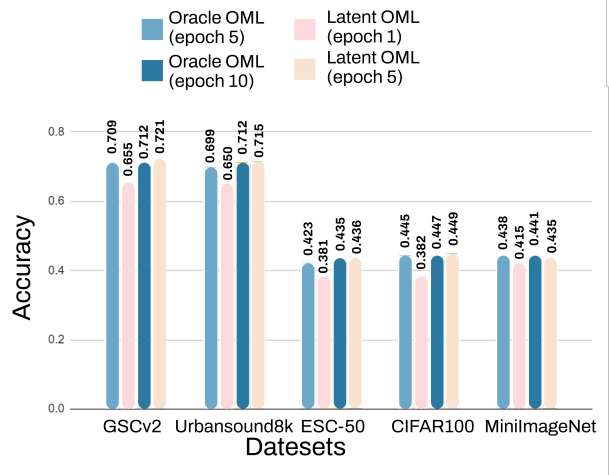
(a) Oracle& Latent under YAMNet architecture



(b) Raw& Latent under YAMNet architecture



(c) ViT architecture



(d) CNN architecture

Figure 9: Comparison of different Meta-CL methods regarding the number of replay epochs.

method attain the same level of accuracy as the Oracle method after five iterations. Additionally, we note that exceeding five iterations does not significantly enhance accuracy. Figures 9band 9c illustrate that the accuracy of Raw OML within the advanced methods surpasses that of the previously tested Latent approach.

C.3 Multi Compression Module.

In CNN architectures, ANML with AIM demonstrates substantial accuracy improvements (26.0% to 34.6% on CIFAR100), albeit with increased memory requirements (39.69MB to 1,093MB). LifeLearner presents an optimal balance between accuracy and memory utilization in resource-constrained environments. The integration of AIM, while beneficial for accuracy, introduces significant computational overhead, particularly in Raw ANML implementations (11,424s latency, 52.5KJ energy consumption on CIFAR100). Oracle ANML offers a compromise between performance enhancement and resource efficiency.

Vision Transformer (ViT) and YAMNet architectures exhibit analogous performance-resource tradeoffs. ViT implementations with OML and AIM show improved accuracy but incur substantial computational costs (22,968s latency, 103KJ energy consumption on CIFAR100). Similarly, YAMNet with AIM achieves superior accuracy (42.9% to 71.0% on GSCv2) at the expense of increased memory utilization (10.16MB to 608.2MB). Pretrained YAMNet models demonstrate superior resource efficiency metrics.

1328 D Extended Related Work

1329 D.1 Continual Learning

1330 Neural network training is difficult to shift from batch learning to a continuous learning model because neural networks are
1331 different from human brain mechanisms. Deep neural network-based systems that are continuously updated with new data suffer
1332 from a severe forgetting problem, where performance on old tasks typically drops significantly, known as CF [McCloskey and
1333 Cohen, 1989; Parisi *et al.*, 2019; Wang *et al.*, 2024; Kwon *et al.*, 2021a; Jha *et al.*, 2021]. Researchers have put forward numerous
1334 approaches to prevent CF, mostly encompassing rehearsal-based, regularization-based, and parameter isolation-based strategies.

1335 (1) Rehearsal-based approaches [Rebuffi *et al.*, 2017; Wu *et al.*, 2019; Chauhan *et al.*, 2020; Kwon *et al.*, 2024a] allow storing
1336 some of the early training data, i.e., old data, in a cache, which will be used for replay or prototype as new tasks are learned
1337 as a way of preventing CF. At this point, cache size, storage data selection, data storage form, and the way old and new data
1338 are mixed are all important influencing factors. Rehearsal-based approaches include memory-based, generation-based replay,
1339 and other approaches. Memory-based approaches generally necessitate a memory buffer for storing data instances or pertinent
1340 information from the previous task. This stored information is then retrieved and utilized during the learning of a new task to
1341 reinforce the knowledge acquired from the prior activity. Rebuffi et al. first proposed a strategy for learning both the classifier and
1342 the feature representations simultaneously during a continuous learning process, which became an incremental classifier(iCARL)
1343 based on representational learning [Rebuffi *et al.*, 2017]. During representation learning, iCARL is trained using a small number
1344 of data instances representative of the old category stored and instances from the new task. Wu et al. suggest that the present
1345 approaches, which demonstrate good performance on small datasets with only a few tasks, are unable to sustain their performance
1346 on huge datasets with thousands of tasks [Wu *et al.*, 2019]. Therefore, they proposed bias-corrected (BIC) methods that focus on
1347 continuous learning from large datasets. Because there is actually a strong bias in the classification layer for each new task, BIC
1348 segregates the validation set from the amalgamation of previous and new data instances and incorporates a linear bias correction
1349 layer subsequent to the classification layer. This correction layer utilizes the validation set to rectify any bias present.

1350 Generative replay-based methods are an alternative to memory-based methods, using generative modules that can reproduce
1351 information related to previous tasks instead of memory buffers. Shin et al. proposed a deep generative replay method (DMC)
1352 that sequentially learns multiple tasks by mimicking pseudo-data generated from previous training examples by a GAN model
1353 and pairing them with corresponding labels [Shin *et al.*, 2017]. Nevertheless, a significant limitation is that the efficacy of the
1354 statement is contingent upon the caliber of the generator. Deep model consolidation (DMC) was proposed by Zhang et al [Zhang
1355 *et al.*, 2020]. The process begins by training a distinct model for the new class using labeled data. Subsequently, the old and new
1356 models are merged by utilizing publicly accessible unlabeled auxiliary data. This approach overcomes the difficulties because of
1357 the inaccessibility of legacy data and mines these auxiliary data for rich transferable representations to facilitate incremental
1358 learning.

1359 Generative replay methods have been shown to be effective on problems with relatively simple inputs, but for more complex
1360 input problems, such as natural images, generative replay methods may face greater challenges. While generative replay still has
1361 some advantages in class incremental learning problems using natural images, these methods rely on pre-trained networks or
1362 extensive non-incremental initialization phases.

1363 (2) Regularization-based approaches [Kirkpatrick *et al.*, 2017; Zenke *et al.*, 2017] usually impose restrictions on various model
1364 parameters and hyperparameters during the updating process to achieve the goal of consolidating knowledge learned in a straight
1365 line while learning a new task, thus mitigating CF in continuous learning. Regularization-based approaches include methods
1366 such as optimizing constraints on important model parameters to add distillation losses with respect to the model as an objective.

1367 A common approach is to enhance the loss function by regularizing previously acquired knowledge, which is a technique that
1368 gained recognition as Enhanced Weight Consolidation (EWC) was first embodied by Kirkpatrick et al. [Kirkpatrick *et al.*, 2017].
1369 EWC introduces a novel quadratic penalty term in the loss function to limit pattern modifications to weights that were more
1370 important for the previous learning task. In order to limit the parameter to low-loss regions that are common between tasks,
1371 instead of only updating low-loss regions for new tasks by calculating the importance of the weights using the diagonal of the
1372 Fisher information matrix [Zamir, 1998], thus mitigating the CF problem. The rebalancing uniform classifier LUCIR method
1373 was proposed by Hou et al. [Hou *et al.*, 2019]. This method proposes three loss functions to bind the bias problem present in
1374 incremental learning due to the imbalance between old and new samples. The data is rebalanced by re-assigning weights in each
1375 iteration cycle. This means that for a few class instances, higher weights will be assigned; for the majority of class instances,
1376 lower weights will be assigned. This reallocation technique ensures that the model pays more attention to the minority class, thus
1377 improving the overall classification performance.

1378 Methods utilizing knowledge distillation [Shin *et al.*, 2017] incorporate the concept of knowledge distillation into incremental
1379 learning by extracting knowledge from a model trained on a previous task into a model trained on a new task, therefore
1380 consolidating previously acquired knowledge. Li et al. proposed a method for learning without forgetting (LWF, Learning
1381 without Forgetting) [Li and Hoiem, 2017]. Prior to acquiring new knowledge, LWF retains a duplicate of the preceding model
1382 parameters. Subsequently, the model acquired from the new task data instances is employed as the classifier target for the old
1383 task. The classifier for the new task is utilized with the objective of attaining the real value. The total of the losses from the new
1384 task and old task is calculated and employed as the ultimate loss. Doulaed et al. refer to continuous learning as representation
1385 learning and propose a distillation loss that becomes a summarized output distillation (POD) [Douillard *et al.*, 2020], which

restricts the updating of the final output and the learned representation of the middle layer. The disadvantage of such methods is that after the first task, all the parameters of the hidden layer are frozen but representation learning is limited. 1386
1387

(3) Parameter isolation-based approaches [Yoon *et al.*, 2017; Mallya and Lazebnik, 2018] typically involve expanding the 1388
old model on new tasks and assigning different model parameters to different tasks with varying degrees of isolation to prevent 1389
subsequent tasks from interfering with previously learned knowledge. 1390

Parameter isolation-based approaches allocate distinct model parameters to individual tasks through the dynamic modification 1391
of the network architecture. Yoon et al. introduced a Dynamically Extensible Network (DEN) [Yoon *et al.*, 2017] that leverages 1392
acquired information from previous jobs and expands the network structure when the existing knowledge is inadequate for 1393
handling new tasks. Neurons undergo processes of addition, duplication, and separation to expand the structure of the network. 1394

In addition to using a parameter isolation-based approach to dynamically change the network architecture, the researchers 1395
also designed a fixed network architecture. This architecture can still assign different parameters to handle different tasks. 1396
Mallya et al. proposed PackNet [Mallya and Lazebnik, 2018], a method that first fixes the parameters of the old task and second 1397
trains the entire neural network for each new task. After the training is completed, unnecessary parameters are released using 1398
weight-based pruning techniques and redundant spatial models are retained. Fernando et al. proposed PathNet [Fernando *et* 1399
al., 2017] which initiates the training process by randomly selecting a few paths within the network. A race selection genetic 1400
algorithm is then employed to choose the most optimal paths for training on the given task. Afterward, for each subsequent task, 1401
the model parameters on all the paths chosen in the prior tasks are locked, while the remaining parameters are reset and trained 1402
again using the aforementioned approach to ultimately achieve the optimal path. Afterward, for each subsequent job, the model 1403
parameters on all the previously selected paths are fixed, while the remaining parameters are reset and trained again using the 1404
aforementioned method in order to ultimately choose the optimal path. 1405

The method based on parameter isolation is simply to cope with the learning of a new task by adding parameters to the original 1406
model, but this method does not eliminate the interference between the new parameters and the old ones, nor does it ensure that 1407
the new parameters will not overwrite the old ones. Therefore, even with the parameter isolation-based approach, incremental 1408
learning is still limited by the problem of CF. 1409

(4) Recently, preserving the structure of previously acquired knowledge has also emerged as a compelling area of research. 1410
Tao et al. proposed the Topology Preserving Class Incremental Learning (TPCIL) approach [Tao *et al.*, 2020] to store resilient 1411
Hebbian graphs [Song *et al.*, 2000] in buffers for data playback effects rather than just stored instances of prior data. TPCIL is 1412
motivated by the concept derived from human cognitive research that the process of forgetting is a result of the destruction of 1413
topological structures in human memory, and the method mitigates CF by injecting topological retention terms into the loss 1414
function. 1415

The 'regularization and parameter isolation based approach' mentioned above sometimes does not work as well as it should. 1416
This is because the approach is not always consistent with new incremental learning and the advantages can even be negative. 1417

D.2 Meta Learning

Meta Learning, also known as few-shot learning, is one of the hotspots of current research. Few-shot learning aims to use few 1419
training samples to recognize new classes that are not concatenable, regardless of the model's performance in recognizing the 1420
base class, and its core problem is that deep models tend to be overfitted to a limited number of training samples [Hospedales *et* 1421
al., 2021]. To mitigate this issue, researchers have proposed a number of methods, which mainly include three main categories: 1422
model-based fine-tuning, data-based enhancement, and migration learning [Wang *et al.*, 2020]. 1423

(1) Meta learning methods [Finn *et al.*, 2017; Arik *et al.*, 2018; Chauhan *et al.*, 2022] based on model fine-tuning are more 1424
traditional approaches, which typically pre-train models on large-scale data and then fine-tune the existing parameters through 1425
regularization. Because of the limited quantity of training samples, how to tune the parameters without leading to overfitting 1426
becomes a key issue, for which the researchers proposed the following solution. a. Early stopping: Arik et al. separated the 1427
validation set from the training set in order to oversee the training process, and the training will cease when there is no discernible 1428
enhancement in the performance of the validation set [Arik *et al.*, 2018]. b. Selective updating of parameters: Keshari and his 1429
team gave a set of pre-trained filters that only learn the parameters that are multiplied by the filters, and this selective updating 1430
of the parameters effectively mitigates overfitting [Keshari *et al.*, 2018]. c. Simultaneous updating of relevant parts of the 1431
parameters: Yoo et al. group the pre-trained neural networks so that the filters are fine-tuned based on some auxiliary information 1432
using the training set via grouped backpropagation for the purpose of jointly updating each grouping using the same update 1433
information [Yoo *et al.*, 2018]. d. Using model regression networks: Kozerawski et al. mapped sample embeddings into a 1434
transformation function for classification decision boundaries [Kozerawski and Turk, 2018]. The model regression network 1435
represents a transformation that is independent of the specific task, which translates parameter values acquired via training 1436
on a limited number of cases to parameter values acquired through training on a substantial number of samples. Although 1437
the model-based fine-tuning approach is simpler, the differences between the source dataset and the target dataset may lead to 1438
overfitting of the model on the target dataset during use. 1439

(2) The fundamental problem of Meta learning is that the sample size is too small, the problem can be supplemented by data 1440
enhancement methods to increase the diversity of the samples and supplement its insufficient number of images. Delta encoders 1441
were proposed by Schwartz et al [Schwartz *et al.*, 2018]. The model can extract transferable intraclass deformations between 1442
training samples of the same class and apply these increments to small samples of the new class, effectively synthesizing new 1443

1444 class samples as it goes. However, in this method, the features usually extracted by the classification network only focus on the
1445 most discriminative regions, while ignoring other less discriminative regions, which is not conducive to the generalization of the
1446 network. To solve this problem, Shen et al. replaced the fixed attention mechanism with an indeterminate one [Shen *et al.*, 2019].
1447 First, the input image is extracted with features, and then the average is pooled and classified to obtain the cross-entropy loss.
1448 This loss is then used to derive the gradient for the uncertain attention mechanism, thus updating the model.

1449 (3) Transfer learning [Yosinski *et al.*, 2014; Kwon *et al.*, 2024b] is the use of knowledge already learned on one task to improve
1450 learning on another task. Its main goal is to quickly transfer what has already been learned to a new domain. a. Metric-based
1451 learning: Vinyals et al. proposed a Matching Network, which maps training samples and validation samples to corresponding
1452 labels [Vinyals *et al.*, 2016]. Then the samples are mapped into a low dimensional vector space using LSTM to compute the
1453 similarity between the new sample and each sample. Finally the predicted labels are output using the kernel density estimation
1454 function. b. Meta learning based approach: Finn et al. proposed a model-independent Model Agnostic Meta Learning (MAML),
1455 aiming at obtaining a good general initialization parameter for the model and achieving fast fine-tuning of the model on new
1456 tasks [Finn *et al.*, 2017]. The strategy learns features that are applicable to a variety of tasks, allowing the model to quickly
1457 adjust the model's weights so that it can be generalized and quickly adapted to new tasks. However, its disadvantage makes it
1458 necessary to train with a sufficient number of tasks to converge. For this reason, Sun et al. proposed Meta Transfer Learning
1459 (MTL) for Few-shot learning. This method enables MAML to learn only the last layer as a classifier [Sun *et al.*, 2019]. It is first
1460 trained on a large-scale dataset to get a full-time deep neural network and fixes the lower-level convolutional layers as feature
1461 extractors. The parameters of the feature extractor neurons are subsequently acquired through learning to ensure their rapid
1462 adaptability to the Few-shot job. When only a small amount of labeled data is used, the method can help deep neural networks
1463 converge quickly and reduce the probability of overfitting occurring. Rusu et al. proposed the LEO method based on MAML to
1464 address the uncertainty of its use of Meta learning [Rusu *et al.*, 2018]. The method first initializes the parameters of the model
1465 for each task. Its parameters are sampled from a conditional probability distribution associated with the training data. Secondly,
1466 the parameters are updated in a low-dimensional hidden space to adapt the model more efficiently.

1467 D.3 Meta Continual Learning

1468 Most of the traditional methods of class Continuous Learning lead to significant performance degradation when applied directly
1469 to Meta-CL. Firstly, because of the limited number of samples in the new class during Meta-CL, the model is prone to overfitting
1470 into the new class, resulting in a loss of its capacity to generalize to large sample tests. Second is the dilemma of facing a
1471 performance tradeoff between the old and new classes. Due to the fact that in the case of very few samples, it is necessary to
1472 increase the learning rate as well as enhance the gradient of the new class loss in order to learn the relevant knowledge of the
1473 new class. However, this will make it more difficult to maintain the relevant knowledge of the old class. Therefore, researchers
1474 address Meta-CL from a new cognitive perspective.

1475 The problem of Meta-CL was raised by Tao et al. [Tao *et al.*, 2020] at first, and they also proposed the TOpology-Preserving
1476 knowledge InCrementer (TOPIC) framework. The original version of the neural network was used for unsupervised learning
1477 during input. To accomplish the Few-shot supervised incremental learning task for each training task, the research team improved
1478 it. The improved supervised neural gas network allows for incremental growth of nodes and edges through competitive learning.
1479 Based on this, this study also designed the neural gas robustness loss function that can effectively suppress the forgetting of
1480 old categories and the neural gas adaptation function that reduces the overfitting in new categories. The TOPIC framework
1481 can alleviate the forgetting of old knowledge by stabilizing the topology of the neural gas network NGs. It also improves
1482 representation learning on a small number of new category samples by making the NG grow [Fritzke, 1994] and adapt to new
1483 training samples to prevent overfitting to new categories with fewer samples.

1484 To solve the Few-shot incremental learning problem, Cheragian et al. proposed a Semantic-aware Knowledge Distillation
1485 approach [Cheraghian *et al.*, 2021]. The main idea is to introduce semantic information in knowledge distillation to accomplish
1486 the preservation of old things in the process of Meta-CL. The method first transforms the labels into word vectors. The input
1487 image is mapped to the space of its label word vectors to minimize the distance between the two vectors. No additional neural
1488 network parameters need to be added as new categories emerge, thus reducing the dependence of network training on the amount
1489 of data. Shi et al. proposed a method based on the discovery of flat minima (F2M) [Shi *et al.*, 2021] for model training in
1490 incremental Few-shot learning. An average minimum is when the model parameters are in a flat region and when the loss
1491 function value is minimized. This flat region prevents the model from overfitting and preserves previously learned knowledge
1492 when learning new data. A Continuous Evolutionary Classifier (CEC) was proposed by Zhang et al [Zhang *et al.*, 2021]. The
1493 method initially separates the feature extraction module from the classifier, where the feature extraction module is frozen to
1494 avoid generating forgetfulness and only the classifier is changed for each incremental task. The process is that whenever vectors
1495 for a new category are generated, the vectors obtained from all categories, old and new, will be aggregated together. Where each
1496 vector is a node and the nodes are aggregated based on an attention mechanism that utilizes the invariance of the connections
1497 between the nodes to maintain the old knowledge. Finally, the graph attention model is utilized to generate the final classifier by
1498 combining the information of the emerged categories. A self-promoting prototype refinement mechanism (SPPR) was proposed
1499 by Zhu et al [Zhu *et al.*, 2021]. The technique uses the correlation matrix between newly introduced category samples and
1500 pre-existing category prototypes to revise the current prototypes. This mechanism is realized by dynamic relational projection.
1501 The heart-tired sample representations and the just-tired prototypes are mapped into the same embedding space, and the two

embeddings are computed in the above-mentioned distance metric in the space to compute the space of projection matrices 1502
between them. Ultimately, this matrix space serves as a weight for prototype refinement to guide the dynamics of the prototypes 1503
toward preserving existing knowledge and enhancing the defensibility of new categories. 1504

Recently, Zhou et al. proposed a Forward Compatible Training (FACT) [Zhou *et al.*, 2022]. It makes it easy to merge new 1505
categories and facilitates the seamless integration of these categories into the existing model. In order to enable the model to 1506
be expandable, they designate many virtual prototypes in advance within the embedding area as reserved space and optimize 1507
these virtual circles to push instances of the same class closer together, thus reserving more space for incoming new classes. 1508
Subsequently, Constrained Few Shot Incremental Learning (C-FSCIL) was proposed by Hersche et al [Hersche *et al.*, 2022]. The 1509
method first creates and updates the average prototype vector so that it serves as the average of the samples in memory. It then 1510
polarizes the prototype vector and retraces the fully connected layer for no more than a constant number of iterations. Finally, the 1511
average prototype vector is pushed so that it is quasi-orthogonal and remains close to the average prototype at the original site. 1512

Table 3: Performance and computational costs, memory footprint of six representative Meta-CL methods using three network architectures on five datasets of image and audio domains. OOM indicates an out-of-memory issue.

Dataset	Method	CNN				ViT			
		Accuracy	Memory	Latency	Energy	Accuracy	Memory	Latency	Energy
CIFAR100	Pretrained	0.260	39.69MB	305s	1.44KJ	0.119	29.8MB	615s	2.96KJ
	ANML	0.272	39.69MB	309s	1.44KJ	-	-	-	-
	ANML+AIM	0.346	1,093MB	6,390s	29.43KJ	-	-	-	-
	OML	-	-	-	-	0.271	29.8MB	628s	3.03KJ
	OML+AIM	0.311	834.1MB	1,481s	6.84KJ	-	-	-	-
	Raw ANML	0.392	99.5MB	11,424s	52.5KJ	-	-	-	-
	Raw OML	-	-	-	-	0.40	153MB	22,968s	103KJ
	Oracle ANML	0.445	39.93MB	1,866s	8.55KJ	-	-	-	-
	Oracle OML	-	-	-	-	0.361	29.5MB	3,672s	19.4KJ
	Lifelearner	0.452	15.45MB	374s	1.71KJ	-	-	-	-
Mini ImageNet	Latent OML	-	-	-	-	0.365	36.8MB	764s	3.76KJ
	Pretrained	0.258	474.5MB	1,198s	5.5KJ	0.234	336.6 MB	2,056s	11.2KJ
	ANML	0.327	474.5MB	1,152s	5.3KJ	-	-	-	-
	ANML+AIM	0.331	1,562 MB	OOM	OOM	-	-	-	-
	OML	-	-	-	-	0.255	336.6 MB	2,203s	11.4KJ
	OML+AIM	0.187	1,051 MB	1,434s	6.5KJ	-	-	-	-
	Raw ANML	0.429	897.1 MB	185,610s	810KJ	-	-	-	-
	Raw OML	-	-	-	-	0.454	1,334 MB	301,456s	1150KJ
	Oracle ANML	0.438	475.0 MB	3,414s	15.7KJ	-	-	-	-
	Oracle OML	-	-	-	-	0.349	337.7 MB	6,301s	31KJ
GSCv2	Lifelearner	0.433	512.5 MB	1,343s	6.17kJ	-	-	-	-
	Latent OML	-	-	-	-	0.376	336.6 MB	2,250s	13KJ
		CNN				YAMNet			
Urban Sound8K	Pretrained	0.213	10.16MB	71.1s	0.324KJ	0.061	39.2MB	213.6s	1.08KJ
	ANML	0.429	10.16MB	71.1s	0.324KJ	-	-	-	-
	ANML+AIM	0.710	608.2MB	394.2s	1.8KJ	-	-	-	-
	OML	-	-	-	-	0.329	39.2MB	209.8s	1.08KJ
	OML+AIM	0.649	135.2MB	157.5s	0.72KJ	-	-	-	-
	Raw ANML	0.135	45.72MB	735.6s	3.37KJ	-	-	-	-
	Raw OML	-	-	-	-	0.749	120MB	1,482s	6.85KJ
	Oracle ANML	0.712	10.20MB	569.7s	2.6KJ	-	-	-	-
	Oracle OML	-	-	-	-	0.701	39.7MB	1,685s	14.6KJ
	Lifelearner	0.713	3.40MB	75.6s	0.35KJ	-	-	-	-
ESC-50	Latent OML	-	-	-	-	0.704	40.9MB	235.8s	0.43KJ
ESC-50	Pretrained	0.182	1,382 MB	2,065s	5.7KJ	0.186	39.2 MB	1,365s	5.4KJ
	ANML	0.596	1,382 MB	1,053s	12.4KJ	-	-	-	-
	ANML+AIM	0.439	2,593 MB	1,098s	4.28KJ	-	-	-	-
	OML	-	-	-	-	0.262	39.2 MB	1,874s	5.36KJ
	OML+AIM	0.385	2,648 MB	167,986s	4.88KJ	-	-	-	-
	Raw ANML	0.667	1,456 MB	1,985s	6.97KJ	-	-	-	-
	Raw OML	-	-	-	-	0.595	139.3 MB	2,965s	7.45KJ
	Oracle ANML	0.710	1,384 MB	1,647s	8.35KJ	-	-	-	-
	Oracle OML	-	-	-	-	0.448	42.4 MB	1,875s	6.36KJ
Urban Sound8K	LifeLearner	0.650	496 MB	2,086s	4.98KJ	-	-	-	-
	Latent OML	-	-	-	-	0.442	39.2 MB	1,624s	4.37KJ
GSCv2	Pretrained	0.196	1,163MB	1,359s	7.2KJ	0.090	39.8MB	4,052s	19.6KJ
	ANML	0.308	1,163MB	1,374s	7.2KJ	-	-	-	-
	ANML+AIM	0.233	2,305MB	OOM	OOM	-	-	-	-
	OML	-	-	-	-	0.135	39.8MB	3,986s	19.6KJ
	OML+AIM	0.181	2,152MB	OOM	OOM	-	-	-	-
	Raw ANML	0.358	5,005MB	OOM	OOM	-	-	-	-
	Raw OML	-	-	-	-	0.577	210.8MB	28,465s	39.6
	Oracle ANML	0.435	1,167MB	4,120s	20.3KJ	-	-	-	-
	Oracle OML	-	-	-	-	0.442	42.5MB	12,473s	84.2KJ
	Latent ANML	0.381	316.3MB	1,445s	7.8KJ	-	-	-	-
	Latent OML	-	-	-	-	0.458	44.3MB	4,536s	7.4KJ